Interaction of Colloidal Particles with Macromolecules: The RISM Integral Equation Theory

P. Khalatur, L. Zherenkova, A. Khokhlov

▶ **To cite this version:**

P. Khalatur, L. Zherenkova, A. Khokhlov. Interaction of Colloidal Particles with Macromolecules: The RISM Integral Equation Theory. Journal de Physique II, 1997, 7 (4), pp.543-582. 10.1051/jp2:1997145 . jpa-00248462

HAL Id: jpa-00248462
https://hal.science/jpa-00248462

Submitted on 4 Feb 2008

HAL is a multi-disciplinary open access archive for the deposit and dissemination of scientific research documents, whether they are published or not. The documents may come from teaching and research institutions in France or abroad, or from public or private research centers.

L'archive ouverte pluridisciplinaire **HAL**, est destinée au dépôt et à la diffusion de documents scientifiques de niveau recherche, publiés ou non, émanant des établissements d'enseignement et de recherche français ou étrangers, des laboratoires publics ou privés.

Interaction of Colloidal Particles with Macromolecules: The RISM Integral Equation Theory

P.G. Khalatur ([1]), L.V. Zherenkova ([1]) and A.R. Khokhlov ([2,*])

([1]) Department of Physical Chemistry, Tver State University, Tver 170002, Russia
([2]) Physics Department, Moscow State University, Moscow 117234, Russia

(Received 15 July 1996, revised 16 December 1996, accepted 7 January 1997)

PACS.61.25.Hq – Macromolecular and polymer solutions; polymer melts; swelling
PACS.82.70.Dd – Colloids

Abstract. — A microscopic theory of the mixtures of polymer chains and colloidal particles immersed in a common solvent is developed on the basis of the RISM integral equation technique. The obtained general equations enable the calculation of the correlation functions and thermodynamic characteristics of the system at an arbitrary ratio of the components. The theory is used for a comprehensive study of interaction of small spherical particles with flexible polymer chains in the regimes of weak and strong adsorption of the macromolecules on the surface of the particles. The temperature and concentration regions characterized by different effect of the polymer on stability of the colloidal dispersion are determined. The corresponding temperature–concentration diagrams of state are constructed.

1. Introduction

One of the important recent trends in chemical technology is a wide use of synthetic and natural polymers as stabilizers for colloid systems (sols, dispersions, microemulsions, micellar solutions, *etc.*) [1–3]. The traditional fields of application of polymer additives are preconcentration and dehydration of suspensions in mineral processing, purification of drinking and waste water, improvement of the filtration characteristics and structure of soil, stabilization of lacquers, dyes, and nutritional and pharmaceutical emulsions, *etc.* Even very small polymer additives can have a crucial effect on the aggregation and kinetic stability of colloids and change their rheological characteristics. Moreover, interaction of macromolecules with colloidal particles can result in formation of thermodynamically stable structures of different types. These structures are of considerable interest on their own. Three different structural types can be defined, namely, colloidal liquids, colloidal aggregates, and colloidal crystals. Normally, the colloidal liquids consist of the positively charged small counterions immersed in water and the negatively charged colloidal particles, with the size ranging from 2–5 nm (typical micelles) to $\sim 10^2$ nm (*e.g.*, polystyrene balls). The colloidal aggregates and their growth processes are at present being actively investigated in connection with fractal structures. As for the colloidal crystals, both natural and synthetic colloidal crystals exist, and these systems sometimes bear a similarity to the classical Wigner crystal.

(*) Author for correspondence (e-mail: khokhlov@polly.phys.msu.su)

© Les Éditions de Physique 1997

Numerous practical applications stimulate development of theoretical approaches for quantitative description of various processes occurring in polymer–containing colloid systems. Consequently, colloid systems containing polymers have been extensively studied by several authors [1–35]. Most of the theories known in the literature are based either on a classical mean–field approximation [5–14,21,22,26,28–30] widely used in the physics of polymer solutions [36] or on a phenomenological scaling concept [4] (see, *e.g.*, Refs. [15–18,20,24,25,27,31,35]). Using both approaches one can consider the behavior of the system only qualitatively. In other words, such theories do not take into account directly the chemical structure of macromolecules and the interaction potentials of polymer segments and colloidal particles. There are several other theories for the interaction of colloidal particles in polymer solutions with and without adsorbed polymer. If we assume that a pair of colloidal particles can be represented by two parallel plates immersed in a solvent, then the simplest model of a problem of this type is a dilute polymer solution that is confined into a thin film between two flat impenetrable surfaces. The statistical behavior of polymer chains confined between solid surfaces has been investigated by many authors [6,13,18,37–49], mostly for diluted solutions. It has been found that at very low polymer densities the effective interaction between the plates is of the order of the size of the polymer coil ($\sim R_g$). At moderate and high polymer densities, however, the interaction between neutral plates induced by polymer chains differs from the interaction in a dilute solution in the sense that the relevant length scale for the polymer–mediated interaction is not the global size of the polymer coil R_g, but rather the diameter of monomeric unit, σ_p [50,51]. This result was obtained first by Yethiraj and Hall [50]. In their study, they used the RISM (reference interaction site model) theory of Curro and Schweizer [52–54] in conjunction with the "growing adsorbent" model of Henderson *et al.* [55] and its extension to slitlike pores by Zhou and Stell [56], to develop an integral equation theory for hard chains placed in slitlike pores. The theory [50] is in good agreement with full many–molecular Monte Carlo simulation data for the density profiles of short hard chains (4–mers and 8–mers) at a smooth hard wall. Using the RISM–wall theory, Schweizer *et al.* [57] have calculated these profiles for a system of long chains. It was concluded [50,51] that at high chain concentrations a correct calculation of the effective potential acting between hard walls in polymer medium must be based on a more realistic model than has been widely used [5–35,37–42], *i.e.*, on a model of polymer chains that includes both the global length scales $\sim R_g$ and the short, monomeric length scales σ_p. In particular, it has been found that the force on surfaces immersed in a polymer solution is an oscillatory function of plate separation at high polymer concentrations, with a period of about one monomeric diameter σ_p. Thus, to understand many of the equilibrium properties of polymers near the surface of hard particles, it is crucial that the structure of polymers be realistically modeled at the molecular level. A second microscopic theory which permits the calculation of the density profiles near a hard wall is the density functional (DF) methodology [58–61]. In the last years, there have been several investigations of the behavior of polyatomic fluids near impenetrable walls using the DF theory [60,62–68]. The weighted DF theory of Woodward [60,67,68] is able to accurately predict the segment density profiles in hard chain/hard sphere mixtures.

The effective interaction between small hard spheres in solutions containing dissolved flexible polymer chains has been investigated by Yethiraj, Hall, and Dickman [51] using the RISM integral equations. The polymer molecules were modeled as freely jointed chains of hard spheres (beads). In this study, the simplest regime was considered when *no* adsorption of chains occurs on the particles. The model therefore focuses on excluded volume effects in the system. In the limit as the colloids become *infinitely* diluted, the effective potential (or potential of mean force) between two colloidal particles immersed in a polymer solution was found. In the present paper we also use the RISM integral equation theory to study the interaction between colloidal

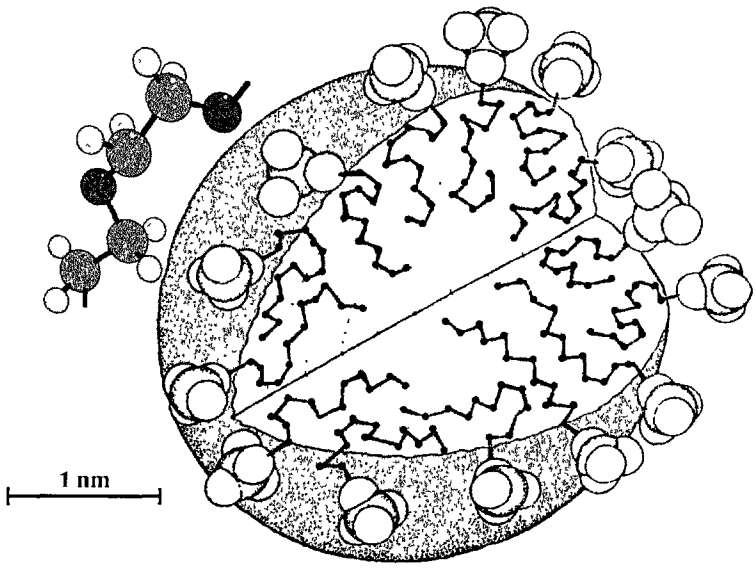

Fig. 1. — Schematic representation of a spherical micelle (a colloidal particle) and a fragment of chain of poly(ethylene oxide). Observance of the proportions between the particle and polymer sizes is approximate. The drawing of micelle is based on calculations by Gruen [73].

particles and macromolecules. The general purposes of our study is:

i) to develop a microscopic theory on the basis of the RISM integral equations which directly takes into account the specific structure and adsorption interactions of the species;

ii) to carry out a detailed study of interaction of flexible polymer chains with colloidal particles, aggregation processes, and properties of structures formed under equilibrium conditions.

The key problem of the theory of polymer-containing colloid systems is the prediction of (a) the types of structures formed as the result of interaction of macromolecules with the particles and (b) the regions of thermodynamic stability (*e.g.*, the temperature and concentration ranges) of different states of the system. In this paper we solve this problem within the framework of the theoretical approach based on the method of integral equations. We will be mainly interested in the consideration of the interaction of flexible polymer chains with small spherical particles of diameter of the order of the Kuhn segment length of a chain. The prototype of our model used is the system studied experimentally in great detail by Cabane and Duplessix [69–73] using small-angle neutron scattering, namely a semidilute aqueous solution of poly(ethylene oxide) (PEO) containing spherical micelles of sodium dodecyl sulfate (SDS) molecules. Figure 1 gives a schematic representation of both components with the indication of the corresponding spatial sizes. In the following discussion of the model and the results we will use both notations "colloidal particle" and "micelle" on equal terms.

In the next section we remind some of the basic equations of the RISM-type theory and derive general RISM equations for the binary system considered in the present paper. The specification of the model and the calculational procedure are described in Section 3. In Section 4, we present and discuss the results obtained. In Section 5, we summarize our results.

2. Integral RISM Equations Describing Polymer-Containing Colloid Systems

First of all, let us remind the fundamentals for the RISM approach for an arbitrary one–component system consisting of identical molecules (particles). We assume that each molecule is a set of N sites, the interaction between which is characterized by the pair potentials $u(r)$. By an interaction site we assume an atom, a single segment (monomer) of a polymer chain, or a colloidal particle. The potential energy of interaction between two molecules 1 and 2 is

$$U(1,2) = \sum_{\alpha=1}^{N} \sum_{\beta=1}^{N} u_{\alpha\beta}(r), \tag{1}$$

where $r = |\mathbf{r}_\alpha - \mathbf{r}_\beta|$ is the distance between two interaction sites α and β; $\mathbf{r}_\alpha$ and $\mathbf{r}_\beta$ are their position vectors; and $u_{\alpha\beta}(r)$ is the corresponding pair potential. In the general case, such description of the system gives the possibility to use the Chandler–Andersen integral matrix RISM equation [74].

$$\mathbf{H}(r) = \int\int \mathbf{W}(|\mathbf{r} - \mathbf{r}'|)\mathbf{C}(|\mathbf{r}' - \mathbf{r}''|)[\mathbf{W}(\mathbf{r}'') + \rho\mathbf{H}(\mathbf{r}'')]\mathrm{d}\mathbf{r}'\mathrm{d}\mathbf{r}''. \tag{2}$$

Here ρ is the number of molecules (particles) per unit volume; $\mathbf{H}$, $\mathbf{C}$, and $\mathbf{W}$ are the $N \times N$ matrices combined of the *inter*molecular site–site total correlation functions, $h(r)$, the corresponding intermolecular direct correlation functions, $c(r)$, and the *intra*molecular probability distribution functions, $w(r)$:

$$\begin{aligned}
\mathbf{H}(r) &= \begin{bmatrix} h_{11}(r) & h_{1N}(r) \\ & \\ h_{N1}(r) & h_{NN}(r) \end{bmatrix}, \\
\mathbf{C}(r) &= \begin{bmatrix} c_{11}(r) & c_{1N}(r) \\ & \\ c_{N1}(r) & c_{NN}(r) \end{bmatrix}, \\
\mathbf{W}(r) &= \begin{bmatrix} w_{11}(r) & w_{1N}(r) \\ & \\ w_{N1}(r) & w_{NN}(r) \end{bmatrix},
\end{aligned} \tag{3}$$

where the correlation functions $h_{\alpha\beta}(r)$, $c_{\alpha\beta}(r)$, and $w_{\alpha\beta}(r)$ refer to a given pair of interaction sites α and β (α, $\beta = 1, 2, \ldots, N$) separated by distance $r = |\mathbf{r}_\alpha - \mathbf{r}_\beta|$.

For a system of single–center (spherical) particles (*i.e.*, at $N \equiv N_\mathrm{d} = 1$ and $w_{\alpha\beta}(r) = 1$) matrix equation (2) is reduced to the usual Ornstein–Zernike equation [75, 76]

$$h(r) = c(r) + \rho \int c(|\mathbf{r} - \mathbf{r}'|)h(\mathbf{r}')\mathrm{d}\mathbf{r}'. \tag{4}$$

Using the symbol $*$ as the notation for integral convolution gives a more convenient compact representation of equations (2) and (4):

$$\mathbf{H}(r) = \mathbf{W}(r) * \mathbf{C}(r) * \mathbf{W}(r) + \rho\mathbf{W}(r) * \mathbf{C}(r) * \mathbf{H}(r), \tag{5}$$

$$h(r) = c(r) + \rho c(r) * h(r). \tag{6}$$

Returning now to the system of polymer chains and colloidal particles, let us divide the problem into two parts. First, we must write the integral equations for each component of this system, *i.e.* for polymer chains and colloidal particles, in the form allowing one to obtain their numerical solution. Second, we must write the equation in the mixed form that takes into account the interaction between the components at their arbitrary ratio.

It is natural to consider the colloid subsystem as a set of single–center spherical particles at a given number density $\rho_d = n_d/V$. where n_d is the number of particles in volume V. In this case, using the subscript dd to identify the corresponding pair correlation for this component, we have

$$h_{dd}(r) = c_{dd}(r) + \rho_d c_{dd}(r) * h_{dd}(r). \tag{7}$$

As for the polymer component, a serious problem arises, because in this case the number of interaction sites is usually very large ($N \equiv N_p \gg 1$) and the initial set of coupled integral equations (2) becomes rather cumbersome. However, in the case of regular polymers it becomes possible to solve this problem by using some approximate description, the accuracy of which increases with the chain length $N \equiv N_p$. The main idea of this approach, which was first used in polymer theory by Schweizer and Curro [77] (see also Refs. [52–54]), is to go from partial site–site correlation functions $h_{\alpha\beta}(r)$, $c_{\alpha\beta}(r)$, and $w_{\alpha\beta}(r)$ to the collective (*molecular*) functions. We will do the same thing, but using different derivation based on the scattering theory. Note that a somewhat similar approach has been applied by Genz *et al.* [78,79] (see also Refs. [80,81]).

Let us rewrite equation (2) in the reciprocal q space. Then, for an arbitrary pair of interaction sites α and β we have

$$\hat{h}_{\alpha\beta}(q) = \sum_{\delta=1}^{N}\sum_{\gamma=1}^{N} \hat{w}_{\alpha\gamma}(q)\hat{c}_{\gamma\delta}(q)\left[\hat{w}_{\delta\beta}(q) + \rho\hat{h}_{\delta\beta}(q)\right], \quad (\alpha,\beta = 1,2,\cdot\ ,N), \tag{8}$$

where $\hat{h}_{\alpha\beta}(q)$, $\hat{c}_{\alpha\beta}(q)$, and $\hat{w}_{\alpha\beta}(q)$ are the Fourier transforms of the corresponding correlation functions; for example,

$$\hat{h}_{\alpha\beta}(q) = \frac{4\pi}{q}\int_0^\infty r h_{\alpha\beta}(r)\sin(qr)\mathrm{d}r. \tag{9}$$

Now, let us recall some facts known from the scattering theory. In the experiments on scattering of particles (*e.g.*, neutrons) the total static structure factor [82]

$$\hat{S}(q) = \hat{w}(q) + \hat{S}^{(m)}(q), \tag{10}$$

is observed, where $q \equiv (4\pi/\lambda)\sin(\theta/2)$ is the absolute value of the wave vector $\mathbf{q}$, θ is the scattering angle, and λ is the de Broglie wave length. In equation (10), the function $\hat{S}^{(m)}(q)$ is associated with the intermolecular scattering and $\hat{w}(q) = N^{-1}\sum_{\alpha,\beta}^{N}\langle\exp[i\mathbf{q}(\mathbf{r}_\alpha - \mathbf{r}_\beta)]\rangle$ is the "intrinsic" contribution of the atoms belonging to the same N–atom molecule (*i.e.*, scattering by the ideal gas of molecules); $\mathbf{r}_\alpha$ and $\mathbf{r}_\beta$ denote the positions of atoms α and β on the same molecule. By definition [82], for a homogeneous system we have

$$\hat{S}^{(m)}(q) = \frac{\sum_{\alpha=1}^{N}\sum_{\beta=1}^{N} b_\alpha b_\beta \hat{a}_{\alpha\beta}(q)}{\sum_{\alpha=1}^{N} b_\alpha^2}, \tag{11}$$

$$\hat{a}_{\alpha\beta}(q) = \frac{4\pi\rho}{q}\int_0^\infty r h_{\alpha\beta}(r)\sin(qr)\mathrm{d}r. \tag{12}$$

Here b_α is the amplitude of scattering by atom α (its scattering length) and $\hat{a}_{\alpha\beta}(q)$ is the partial structure factor of a given pair of atoms. Note that as long as the size of atom α is smaller than the inverse scattering vector $1/q$, the q–dependence of b_α can be neglected. As can be seen from equations (9) and (12), $\hat{a}_{\alpha\beta}(q) = \rho\hat{h}_{\alpha\beta}(q)$. For $\hat{w}(q)$, the well–known Debye equation [82] is valid:

$$\hat{w}(q) = \frac{\sum_{\alpha=1}^{N}\sum_{\beta=1}^{N} b_\alpha b_\beta \hat{w}_{\alpha\beta}(q)}{\sum_{\alpha=1}^{N} b_\alpha^2}, \tag{13}$$

$$\hat{w}_{\alpha\beta}(q) = \frac{\sin(ql_{\alpha\beta})}{ql_{\alpha\beta}}, \tag{14}$$

where $l_{\alpha\beta}$ is the equilibrium distance between atoms α and β in a molecule. In this paper we assume that scattering occurs from segments and all $N \equiv N_\mathrm{p}$ polymer segments, or monomers, of a polymer chain are identical ($b_1 = b_2 = \ .. = b_\mathrm{N}$). In addition, we will assume that the pair correlation functions between monomers do not have any angular dependencies, so that our treatment is restricted to polymers having a coiled configuration. Thus the monomers themselves will be considered to be spherical particles. Then, we can write

$$\hat{S}(q) = \frac{1}{N}\sum_{\alpha=1}^{N}\sum_{\beta=1}^{N}\left[\hat{w}_{\alpha\beta}(q) + \rho\hat{h}_{\alpha\beta}(q)\right] \equiv \frac{1}{N}\sum_{\alpha=1}^{N}\sum_{\beta=1}^{N}\hat{S}_{\alpha\beta}(q), \tag{15}$$

$$\hat{w}(q) = \frac{1}{N}\sum_{\alpha=1}^{N}\sum_{\beta=1}^{N}\hat{w}_{\alpha\beta}(q). \tag{16}$$

The function $\hat{S}(q)$ is a typical example of a *molecular* correlation function. From the formal point of view, this function is the result of averaging over partial contributions $\hat{S}_{\alpha\beta}(q) \equiv \hat{w}_{\alpha\beta}(q) + \rho\hat{h}_{\alpha\beta}(q)$. Note that $\hat{S}(q)$ is directly observed in an experiment, and it is precisely *via* this function the main thermodynamic characteristics of the system can be expressed (in particular, for isothermal compressibility we have: $\chi_\mathrm{T} = (1/k_\mathrm{B}T\rho)\lim_{q\to 0}\hat{S}(q)$).

The function $\hat{w}(q)$ is also the *molecular* function averaged over partial contributions $\hat{w}_{\alpha\beta}(q)$. Taking into account equation (15), we rewrite equation (8) as

$$\hat{h}_{\alpha\beta}(q) = \sum_{\delta=1}^{N}\sum_{\gamma=1}^{N}\hat{w}_{\alpha\gamma}(q)\hat{c}_{\gamma\delta}(q)\hat{S}_{\delta\beta}(q) \quad (\alpha,\beta = 1,2,\cdot\ \ ,N). \tag{17}$$

Now let us rewrite this equation in terms of the molecular structure factors $\hat{S}(q)$ and $\hat{w}(q)$. In other words, the particular values of the individual contributions $\hat{S}_{\alpha\beta}(q)$ and $\hat{w}_{\alpha\beta}(q)$ are of no further interest to us; the only requirement is that they give correct values of sums in equations (15) and (16). On the basis of the previous consideration, it is natural to suppose that in the system of sufficiently long chains ($N_\mathrm{p} \equiv N \gg 1$), all the segments of which are identical, each segment gives the same contribution to $\hat{S}(q)$ and $\hat{w}(q)$. Therefore, we can write

$$\hat{S}_{\alpha\beta}(q) = \frac{1}{N}\hat{S}(q), \tag{18}$$

$$\hat{w}_{\alpha\beta}(q) = \frac{1}{N}\hat{w}(q). \tag{19}$$

It is easy to show that substitution of equations (18) and (19) into equations (15) and (16). respectively, gives mathematically identical expressions. Using definitions (18) and (19), we rewrite equation (17) in the form

$$\hat{h}_{\alpha\beta}(q) = \frac{1}{N^2}\hat{w}(q)\left[\sum_{\delta=1}^{N}\sum_{\gamma=1}^{N}\hat{c}_{\gamma\delta}(q)\right]\hat{S}(q), \quad (\alpha,\beta = 1,2,\cdot\ ,N). \tag{20}$$

Next, by analogy with equations (15) and (16) the molecular correlation functions $\hat{h}(q)$ and $\hat{c}(q)$ can be introduced (see also Ref. [77]):

$$\hat{h}(q) = \frac{1}{N^2}\sum_{\delta=1}^{N}\sum_{\gamma=1}^{N}\hat{h}_{\alpha\beta}(q), \tag{21}$$

$$\hat{c}(q) = \frac{1}{N^2}\sum_{\delta=1}^{N}\sum_{\gamma=1}^{N}\hat{c}_{\alpha\beta}(q). \tag{22}$$

In this case we also do not consider the individual partial functions $\hat{h}_{\alpha\beta}(q)$ and $\hat{c}_{\alpha\beta}(q)$ but take into account only their averaged sums. It is these values that are closely related to the main experimentally observed characteristic $\hat{S}(q)$. Now, by summing equation (20) over α and β and using equations (21) and (22), we reduce the initial multicenter RISM equation (2) to a one–dimensional integral equation

$$\hat{h}(q) = \hat{w}(q)\hat{c}(q)\hat{w}(q) + N\rho\hat{w}(q)\hat{c}(q)\hat{h}(q). \tag{23}$$

Finally, using the subscripts p and pp to identify density and correlation functions of the polymer component and performing the inverse Fourier transform of equation (23), we obtain:

$$h_{\mathrm{pp}}(r) = w_{\mathrm{pp}}(r) * c_{\mathrm{pp}}(r) * w_{\mathrm{pp}}(r) + \rho_{\mathrm{p}} w_{\mathrm{pp}}(r) * c_{\mathrm{pp}}(r) * h_{\mathrm{pp}}(r), \tag{24}$$

where $\rho_{\mathrm{p}} = N_{\mathrm{p}}\rho$. This equation coincides with the so–called PRISM equation obtained for the first time by Schweizer and Curro [77] on the basis of some other considerations (not related to the scattering theory).

The change from partial correlation functions to the averaged molecular functions has a rather clear physical sense. In fact, by doing so we assume that in the case of a long polymer chain the end effects are small, internal (nonterminal) segments are all equivalent to each other, and correlations between any arbitrary two segments belonging to the same chain (or two different chains) are determined only by the distance between these segments but not by their positions in the chain (chains). Apparently, this assumption was used when we performed averaging over all segments. One can find a precise estimate for the inaccuracy of such an approximation. As was shown using the perturbation theory [52], the first–order correction to the molecular functions (21) and (22) is proportional to N^{-2} and the expression for $\hat{w}(q)$ in equation (23) is precise. Therefore, in the case $N \gg 1$ we can ignore the inaccuracy appearing in going from equation (2) to equation (24). Thus, we have two one–dimensional integral equations (7) and (24) that characterize behavior of the two individual components.

Our next problem is to write a system of coupled integral equations that would describe interaction between the polymer component and the colloidal particles. To take into account correlations of the "polymer–particles" type, in the general case it is necessary to introduce

two additional types of total correlation functions, which will be further denoted as $h_{dp}(r)$ and $h_{pd}(r)$. Similarly we introduce the "mixed" direct correlation functions $c_{dp}(r)$ and $c_{pd}(r)$. From the complete set of correlation functions we combine the matrices

$$\mathbf{H}(r) = \begin{bmatrix} h_{dd}(r) & h_{dp}(r) \\ h_{pd}(r) & h_{pp}(r) \end{bmatrix}, \quad \mathbf{C}(r) = \begin{bmatrix} c_{dd}(r) & c_{dp}(r) \\ c_{pd}(r) & c_{pp}(r) \end{bmatrix}. \tag{25}$$

For generality, we will use the function $w_{dd}(r)$, which is equal to unity everywhere in the system considered. From the functions $w(r)$ and densities ρ_d and ρ_p we combine two diagonal matrices

$$\mathbf{W}(r) = \begin{bmatrix} w_{dd}(r) & 0 \\ 0 & w_{pp}(r) \end{bmatrix}, \quad \mathbf{D}^{1/2} = \begin{bmatrix} \sqrt{\rho_d} & 0 \\ 0 & \sqrt{\rho_p} \end{bmatrix}. \tag{26}$$

Using equations (25) and (26), we can write the following integral matrix equation

$$\mathbf{D}^{1/2}\mathbf{H}\mathbf{D}^{1/2} = \mathbf{W} * (\mathbf{D}^{1/2}\mathbf{C}\mathbf{D}^{1/2}) * \left[\mathbf{W} + \mathbf{D}^{1/2}\mathbf{H}\mathbf{D}^{1/2}\right]. \tag{27}$$

At $\rho_d \neq 0$ and $\rho_p \neq 0$ we have

$$\mathbf{H} = \mathbf{W} * \mathbf{C} * [\mathbf{W} + \mathbf{D}\mathbf{H}]. \tag{28}$$

Below we present the formal solution of this equation in the reciprocal q space (see also Ref. [83])

$$\hat{h}_{dd} = \frac{1}{\Delta}\hat{w}_{dd}\left[\hat{c}_{dd}\left(1 - \rho_p\hat{w}_{pp}\hat{c}_{pp}\right) + \rho_p\hat{c}_{dp}\hat{w}_{pp}\hat{c}_{pd}\right]\hat{w}_{dd}, \tag{29a}$$

$$\hat{h}_{pd} = \frac{1}{\Delta}\hat{w}_{pp}\hat{c}_{pd}\hat{w}_{dd}, \tag{29b}$$

$$\hat{h}_{dp} = \frac{1}{\Delta}\hat{w}_{dd}\hat{c}_{dp}\hat{w}_{pp}, \tag{29c}$$

$$\hat{h}_{pp} = \frac{1}{\Delta}\hat{w}_{pp}\left[\hat{c}_{pp}\left(1 - \rho_d\hat{w}_{dd}\hat{c}_{dd}\right) + \rho_d\hat{c}_{pd}\hat{w}_{dd}\hat{c}_{dp}\right]\hat{w}_{pp}. \tag{29d}$$

where the determinant of system (28) is

$$\Delta = \left(1 - \rho_d\hat{w}_{dd}\hat{c}_{dd}\right)\left(1 - \rho_p\hat{w}_{pp}\hat{c}_{pp}\right) - \rho_d\rho_p\hat{w}_{dd}\hat{c}_{dp}\hat{w}_{pp}\hat{c}_{pd}. \tag{30}$$

One can get the actual solution if the relation, $c(r) = \varphi[h(r), u(r)]$, between the direct correlation functions $c(r)$, the total correlation functions $h(r)$, and the pair site–site potentials $u(r)$ is given. Several such closure relations are known [75, 76]. Substitution of the Fourier transform ($c(r) \overset{F}{\Longrightarrow} \hat{c}(q)$) of these relations into equations (29) and (30) gives the closed system of integral equations with respect to the set of the total pair correlation functions of interest (*i.e.*, $\{h_{ij}(r);\ i, j = d, p\}$). For example, the Percus–Yevick closure [75, 76] gives

$$c_{ij} = [h_{ij}(r) + 1]\frac{f_{ij}(r)}{f_{ij}(r) + 1}, \quad (i, j = d, p) \tag{31}$$

where $f_{ij}(r) = \exp\{-u_{ij}(r)/k_BT\} - 1$ is the Mayer function. As can be seen, using equation (31) or similar relations (*e.g.*, those corresponding to the hypernetted chain approximation) leads to the system of nonlinear integral equations, which, in the general case, can be solved only numerically. The macroscopic parameters (*i.e.*, temperature T and densities ρ_d and ρ_p), interaction potentials u_{dd}, u_{pp}, and $u_{dp} = u_{pd}$, and unimolecular correlation function $w_{pp}(r)$, which takes into account the structural characteristics of a single polymer chain (*i.e.*, its length N_p and geometric and conformational parameters), must be given as well.

3. Model of the System and Method of Calculation

Let us consider the colloidal particles as mutually impenetrable hard spheres of diameter σ_d and assume that volume V contains n_d particles at average number density $\rho_d = n_d/V$ (*i.e.*, at volume fraction of the particles $\Phi_d = \pi\sigma_d^3\rho_d/6$).

Each macromolecule is modeled as a freely jointed chain consisting of a given number N_p of segments linked by $N_p - 1$ bonds of fixed length l. Note that in a freely jointed chain each segment is equivalent to a statistical Kuhn segment. The segment diameter is σ_p. In the following discussion all lengths are given in the units of σ_p. The main parameter in our calculations is the average density of polymer segments in the system ρ_p (or their volume fraction $\Phi_p = \pi\sigma_p^3\rho_p/6$). The relation between the amounts of segments and particles is defined as ρ_p/ρ_d.

We do not directly account for the low-molecular solvent (liquid medium). It is assumed that the presence of the solvent manifests itself only indirectly by affecting the interactions of the colloidal and polymer components of the system. In fact, such a consideration implies the absence of any specific interactions with participation of the solvent molecules and description of the solvent as a continuous medium (which is justified when the size of the corresponding molecules σ_s is much less than σ_d and σ_p). Note that the direct account for the solvent molecules presents no difficulties in the RISM theory; however, the final equations are cumbersome and their numerical analysis becomes rather complicated.

To formulate the model, it is necessary to choose the particle–particle, polymer–polymer, and particle–polymer interaction potentials, u_{dd}, u_{pp}, and u_{dp}. Although the theory of integral equations does not constrain the choice of the type of the functions u_{dd}, u_{pp}, and u_{dp}, in this work we restrict our consideration to the potentials of the simplest types, which, however, account for the most substantial features of real systems. As u_{dd} and u_{pp} we take the simplest hard-sphere potentials

$$u_{dd}(r) = \begin{cases} \infty, & \text{if} \quad r < \sigma_d \\ 0, & \text{if} \quad r \geq \sigma_d \end{cases}, \quad u_{pp}(r) = \begin{cases} \infty, & \text{if} \quad r < \sigma_p \\ 0, & \text{if} \quad r \geq \sigma_p \end{cases}, \tag{32}$$

where r is the distance between the corresponding sites. Interaction of the polymer segments with the colloidal particles is described by the potential of the type hard sphere + rectangular well

$$u_{dp}(r) = \begin{cases} \infty, & \text{if} \quad r < \sigma_{dp} \\ \epsilon_{dp}, & \text{if} \quad \sigma_{dp} \leq r \leq \sigma_{dp} + \Delta \\ 0, & \text{if} \quad r > \sigma_{dp} + \Delta, \end{cases} \tag{33}$$

where $\sigma_{dp} = (\sigma_d + \sigma_p)/2$; Δ is the width of the potential well (or the radius of action of the potential); and ϵ_{dp} is the energy parameter that accounts for the adsorption effects.

Let us give some comments to the set of the parameters chosen. The approximation used for u_{dd} corresponds to the limiting case when the effective Hamaker constant, which characterizes the van der Waals interaction of the particles, is disregarded. In practice, such a situation occurs for example for ionic micelles or for ion-stabilized dispersions when repulsion of double electrical layers prevails. In these cases the pure colloidal dispersion itself (without any additives) is always stable. In other words, the second virial coefficient

$$B_{dd} = 2\pi \int_0^\infty \left\{ 1 - \exp\left[-\frac{u_{dd}(r)}{k_B T} \right] \right\} r^2 dr, \tag{34}$$

which completely determines the behavior of the pure colloid system at small $\rho_d \sim 0$, takes only positive values. In our model, the condition $B_{pp} > 0$, where B_{pp} is written by analogy

with equation (34), is always fulfilled for the pure polymer component as well. In the theory of polymer solutions [36], this condition corresponds to a thermodynamically good solvent quite compatible with a given polymer. Because it is the values B_{dd} and B_{pp} that characterize equilibrium properties of the individual components, one can assume that the particular type of the potential is not essential in solving the general questions formulated above. It is reasonable also to consider the values B_{dd} and B_{pp} as fixed parameters that describe the interactions not in vacuum but in a given solvent. Similar consideration is true for the adsorption potential u_{dp}; the important features in this case are also not the particular type of the potential or the specific values of the parameters ϵ_{dp} and Δ but the sign and value of the corresponding virial coefficient B_{dp}. Apparently, unlike B_{dd} or B_{pp}, at $\epsilon_{dp} \neq 0$ and $\Delta > 0$ the virial coefficient B_{dp} is temperature dependent. The only reasonable restriction to u_{dp} is that the adsorption potential must be a short–range one ($\Delta \sim \sigma_p$). In our calculations the width of the adsorption well Δ is taken equal to the radius of a polymer segment ($\Delta = \sigma_p/2$) and the well depth is $\epsilon_{dp} = -1$ (in units of k_BT).

The relation between the characteristic sizes σ_d and σ_p is of vital importance. Usually, the simplest limiting case $\sigma_d/\sigma_p \to \infty$ is considered in the theories of polymer–containing dispersions, *i.e.*, it is assumed that macromolecules are found in the gap between two plane–parallel plates that model the surface of colloidal particles [6, 13, 18, 37–49]. The situation when σ_d and σ_p are comparable is much more complicated. However, this case is closer to reality. We find estimations for the values σ_d and σ_p using the results of reference [69], where adsorption of PEO on ionic micelles of sodium dodecyl sulfate is studied. The average size of the micelles is about 2 nm. To avoid the complications of the problem of micelle formation and of their equilibrium size and shape, we discuss polymer adsorption on solid spheres of given diameter. The typical size of the statistical segment of flexible polymers (including PEO) is about 1 nm. Because in our case a segment of a macromolecule is equivalent to the statistical segment, we assume that $\sigma_d/\sigma_p = 2$. From similar considerations, the bond length of a model chain is taken equal to $l = \sigma_p$. Figure 1 gives a schematic representation of the real analog of the model considered in the present paper.

For a mixture of macromolecules and colloidal particles we have the integral matrix equation (27), where $w_{dd} = 1$ and the intrachain correlation function $w_{pp}(r)$ describes the specific features of a particular model. In the case of identity of all segments, this function takes the form

$$w_{pp}(r) = \frac{1}{N_p} \sum_{\alpha=1}^{N_p} \sum_{\beta=1}^{N_p} w_{\alpha\beta}(r), \tag{35}$$

where $w_{\alpha\beta}(r)$ is given by [84,85]

$$w_{\alpha\beta}(r) = \delta(r - r_{\alpha\beta})/4\pi r_{\alpha\beta}^2. \tag{36}$$

Here $r_{\alpha\beta} = |\mathbf{r}_\alpha - \mathbf{r}_\beta|$ and $\delta(r)$ is the Dirac delta function. In the reciprocal q space the Fourier transform of $w_{\alpha\beta}(r)$ gives $\hat{w}_{\alpha\beta} = \sin(qr_{\alpha\beta})/qr_{\alpha\beta}$. For a freely jointed chain with a fixed bond length, l, considered here ([1]), we have: $r_{\alpha\beta} = l(|\alpha - \beta|)^{1/2}$ Then, summation over the indices

([1]) In the literature, the term *freely jointed chain* is sometimes used to describe a *random–flight chain* in which each bond has a constant length l (neglecting the deviation of the length of a bond from its mean value l due to atomic vibrations) (see Ref. [85], page 11). Here we use the term *freely jointed chain* as Flory does [Flory P.J., Statistical Mechanics of Chain Molecules (New York, Interscience Publishers, J.Wiley & Sons, 1969) chap. 8].

α and β of the individual intrachain contributions $\hat{w}_{\alpha\beta}(q)$ gives [84,85]

$$\hat{w}_{\mathrm{pp}}(q) = \frac{1 - \hat{w}^2 - 2\hat{w}N_{\mathrm{p}}^{-1}(1 - \hat{w}^{N_{\mathrm{p}}})}{(1 - \hat{w})^2}, \tag{37}$$

where $\hat{w} = \sin(ql)/ql$. The inverse Fourier transform of $\hat{w}_{\mathrm{pp}}(q)$ gives $w_{\mathrm{pp}}(r)$. Using this function and the Percus–Yevick closure (see Eq. (31)) we have a closed set of coupled nonlinear integral equations (27) with respect to $h_{\mathrm{dd}}(r)$, $h_{\mathrm{dp}}(r) = h_{\mathrm{pd}}(r)$, and $h_{\mathrm{pp}}(r)$. These functions completely define the pair radial density distribution functions of the colloidal particles or polymer segments, $g_{\mathrm{ij}}(r) = h_{\mathrm{ij}}(r) - 1$.

Let us give some comments to the approximations and assumptions adopted in our study:

(i) The use of equation (37) for the intramolecular pair correlation function corresponds to the assumption that intramolecular excluded volume effects can be ignored on all length scales. This assumption is in–line with the so–called ideality principle of Flory [36] which states that for flexible–chain polymers in the melt the equilibrium chain configuration is determined only by intrachain short–range effects, *i.e.*, the *intra*chain and *inter*chain excluded volume interactions effectively cancel. The use of the ideal form (37) for $\hat{w}_{\mathrm{pp}}(q)$ is a crucial step in our treatment, because it decouples the intramolecular and intermolecular correlations and affords a great simplification in the implementation of the RISM theory since the $\hat{w}_{\mathrm{pp}}$ function can be obtained separately without having to calculate it in a self–consistent manner with the intermolecular correlations. On the other hand, the information on the single polymer behavior while interacting with other molecules, is lost. Strictly speaking, the kind of factorization adopted here for the intra– and intermolecular correlations in diluted and moderately concentrated polymer solutions may be justified in the case when the temperature T is taken as very close to the one producing the collapse transition of the chain, and it is assumed to be slightly higher than the Θ–temperature of the polymer/solvent pair, *i.e.*, $(T - \Theta)/T > 0$. The same situation may be realized by suitable choice of a single (or mixed) solvent for a given polymer. In this case, the coupled problem of intrachain and interchain correlations is simplified by constructing the single–polymer form factor, $\hat{w}_{\mathrm{pp}}(q)$, separately, taking the influence of other chains and of colloidal particles into account in an approximate way. It should be noted that the general RISM theory of the structure of flexible molecules in condensed phases has been developed by Chandler *et al.* [86–89], who have introduced an effective self–consistent solvation potential such that the equilibrium conformation of a single solute molecule in its own internal potential plus this solvation potential is approximately the same as the conformation of the same molecule surrounded by solvent molecules in full many–molecular system. The generalization of the polymer RISM approach to self–consistently determined intrachain and interchain pair correlation functions has also been initiated (see. for example, Refs. [53,54,90–95]), but this is still a very difficult task. Among the difficulties appearing here the following ones are the most serious. First, medium–induced two–site solvation potentials (the "hypernetted–chain–style" solvation potential [88, 89] and the "Percus–Yevick–style" solvation potential [92]) proposed in the literature are approximate only. Second, in the case of polyatomic molecules, there is the deviation from pairwise additivity for the total N–site intramolecular solvent–mediated potential of mean force [86–89, 92]. Taking into account these difficulties, we decouple the intramolecular and intermolecular correlations. Thus, in the framework of the approximation used in the present paper, the theory loses its self–consistency, but, as the problem is very complex, this approximation is considered to be an appropriate starting point. The results obtained on the basis of the self–consistent formulation of the polymer–RISM integral theory for polymer–containing colloid systems will be considered in a separate publication [96].

(ii) In order to solve the RISM equation (27) we employ the atomic Percus–Yevick (PY) closure (31). This site–site closure is perhaps the most widely used for systems consisting of unconnected atoms [75,76]. Also there are other closure relations, such as mean spherical approximation (MSA), hypernetted chain approximation (HNC), *etc.* Atomic–like closures have been found [75,76,97] to yield quite good results for homogeneous systems without attractive interactions between chain beads or with relatively short ranged, weak attractions. Recently, however, it has been argued [98,99] that the attempts to use the atomic site–site closures to describe the molecular weight dependence of the critical solution temperature of binary polymer blends give results which are inconsistent with classical mean–field predictions [36] and experimental data. Further, it has been found that all the standard RISM approximations have no correct limiting form at low density limit [100]. Two types of approaches have been proposed in order to overcome these difficulties. One is the so–called RISM–2 theory based on the method of functional Tayler expansion [101,102], which is analogous to the method for simple fluids. Another is the formulation of new "molecular" closures [53,54,98,99], which are apparently correct some of the deficiencies of the standard RISM theory. These closures predict a linear dependence of the critical temperature as a function of the degree of polymerization, in agreement with classical mean field theory [36] and computer simulations. The construction of the RISM–2 theory and the molecular closures is not based on the site–site correlation functions, but on the two–molecule counterpart [53,54,98,99,101,102]. It should be noted, however, that the "usual" closure relations (PY, HNC, MSA) give often quite reasonable results. For instance, Yethiraj and Hall [50] studied the adsorption of hard chains in slitlike pores *via* the wall–polymer–RISM theory in which the wall–polymer and polymer–polymer correlations were treated using the site–site PY closure relations; it was shown that the theory predicts fairly accurately the partition coefficient and the adsorption isotherms for polymer chains. The same approach was successfully used by Yethiraj, Hall, and Dickman [51] to determine the potential of mean force between two small colloidal particles immersed in a polymer solution. Recently, Gromov and de Pablo [103] used the RISM theory to predict the structure of binary polymer blends. In this study, theoretical radial distribution functions $g(r)$ were compared to those obtained from many molecular Monte Carlo simulations of mixtures of Lennard–Jones chains. For the systems of attractive polymer chains Gromov and de Pablo did not find a significant difference between the results obtained with molecular and atomic closures. (Note, however, that such differences could become noticeable at temperatures below those investigated in their work.) Bearing in mind the facts presented above and taking into consideration that the search of the "most accurate" molecular closures remains a topical problem [53,54], we prefer to use the "usual" PY crosure relation (31). It seems that this approximation will give quite acceptable results when the temperature is not too low.

The calculations were performed by iterations using the algorithm described previously in references [104] and [105]. In this algorithm, the Newton–Raphson scheme is combined with the relaxation method. The solution was found in the distance range from 0 to $51.2\sigma_p$. The convolution integrals needed were evaluated *via* fast Fourier transform (FFT) techniques on a grid of $L = 2^{10}$ points equally spaced of $\Delta r = 51.2\sigma_p/L$. The relative accuracy of convergence of the iteration procedure was not lower than 10^{-5} When this accuracy was not achieved, we assumed that no solution existed under the given conditions.

4. Results of Calculations and their Discussion

4.1. Characteristics of the Individual Components. — The aim of this subsection is to relate the spatial sizes of our model system to the real system studied by Cabane and Duplessix [69].

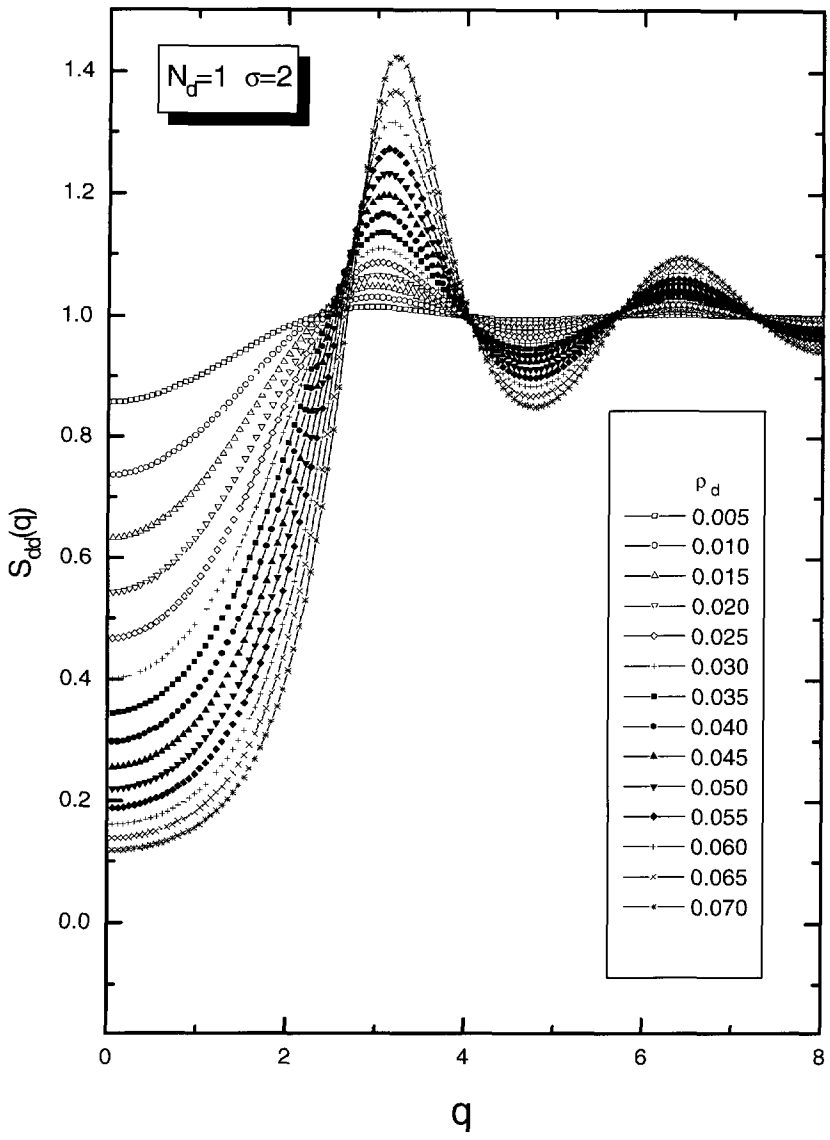

Fig. 2. — Static structure factor of a one–component system of colloidal particles at different densities. The value of q is given in units of $1/\sigma_p$, where σ_p is a characteristic size of the statistical segment (which in our case coincides with a chain segment) of a polymer chain. Diameter of a spherical particle is $2\sigma_p$. Interaction of colloidal particles is described by the hard–sphere potential.

One of the main characteristics observed in experiments on light or neutron scattering is the static structure factor $\hat{S}(q)$. In the case of scattering by point centers (spherical particles) we have: $\hat{S}(q) = 1 + \rho\hat{h}(q)$, where $\hat{h}(q)$ is the Fourier transform of the total correlation function, and r is the average number density of scattering centers.

Figure 2 presents the function $\hat{S}_{dd}(q)$ calculated for a one–component system of colloidal particles at different densities ρ_d. As can be seen, at sufficiently large ρ_d (when the volume

fraction $\Phi_d \gtrsim 0.1$) the structure factor has an oscillating character typical for dense fluids. Let us compare the results of calculation with the experimental data on the properties of a micellar system without polymer additives. In reference [69], the parameter $\sigma_d^3\rho_d$ was about $\sim 10^{-1}$ Comparison of the structure factor obtained in reference [69] with the one calculated at $\sigma_d^3\rho_d = 0.16$ ($\rho_d = 0.02$) shows that both functions are in general close to each other. The exception is the region of small $q \sim 0$. In this region, the experiment [69] gives smaller values for $\hat{S}_{dd}$. This can be explained by the presence, in the real system, of the electrostatic forces of intermicellar repulsion, which reduce the compressibility of the system $\chi_T = (1/k_BT\rho_d) \lim_{q\to 0} \hat{S}_{dd}(q)$. We do not take into account this interaction in order to simplify interpretation of the results. In addition to this, as is mentioned in reference [69], for the system studied the electrostatic repulsion is not sufficiently strong to form ordered array of micelles. In fact, micelles can move sufficiently freely and the first maximum of the function $\hat{S}_{dd}(q)$ at $q = q_1$ is not a small-angle Bragg peak but a usual liquid structure peak characterizing statistical local order. In our model, the origin of the first peak of the structure factor is the same. According to reference [69], average intermicellar distance, $\langle r\rangle = 2\pi/q_1$, is about 10 nm or $\approx 2.5\sigma_d$. Calculations at $\rho_d = 0.01 - 0.02$ give approximately the same estimate for $\langle r\rangle$. The results discussed in the following subsections are obtained at $\rho_d = 0.02$.

Figure 3 presents the correlation functions $\hat{S}_{pp}(q)$ and $g_{pp}(r)$ for the individual polymer component at the number of segments in a chain $N_p = 1000$. Note that in the case when scattering centers are linked in a chain we have: $\hat{S}_{pp}(q) = \hat{w}_{pp}(q) + \rho_p\hat{h}_{pp}(q)$, where $\hat{w}_{pp}(q)$ plays the role of a form factor that characterizes scattering by segments of a single chain ([2]). Apparently, as follows from equation (37), $\hat{S}_{pp} \to N_p$ at $\rho_p \to 0$ and $q \to 0$.

Let us consider first the pair correlation function $g_{pp}(r)$. As can be seen, in a sufficiently large interval of the interchain distances, r, this function is considerably less than unity. Decrease in $g_{pp}(r)$ at small values of r can be explained by mutual repulsion of the parts of chains in thermodynamically good solvent. The characteristic length, ξ, of the function $g_{pp}(r)$, which determines the scale of correlation effects, decreases with the increase in ρ_p. However, at all ρ_p considered here the value of ξ remains large enough. Such a behavior is typical for semidilute polymer solutions [4].

It is convenient to use double-logarithmic coordinates for the analysis of the polymer function $\hat{S}_{pp}(q)$. As follows from comparison of Figures 2 and 3, even at maximum volume fraction of segments studied here ($\Phi_p = 0.419$) the reduced isothermal compressibility $\chi^* = k_BT\rho\chi_T \equiv \hat{S}(0)$ observed for the polymer system is considerably higher than that for the system of particles. This fact is connected with the possibility of interpenetrating of polymer coils. Also note that application of RISM theory to dense polymer systems tends to give predictions for χ^* which are too high [53,54]. This is due in part to the fact that intramolecular chain overlap is allowed in the freely jointed chain correlation function (37). As a result, the effective packing fraction of chain beads is smaller than in the real system. This deficiency can be approximately corrected by artificially using higher polymer densities to increase the effective volume fraction of chain segments [84]. For the freely jointed chains the resulting effective mean monomer packing fraction is $\Phi_p = (\pi/6)\sigma_p^3\rho_p(1 - \kappa_N)$, where $\kappa_N \approx 0.22$ is the fractional overlap volume [84].

At very small ρ_p, the dominant contribution to $\hat{S}_{pp}(q)$ is the intramolecular form factor $\hat{w}_{pp}(q)$, which behaves as $\hat{w}_{pp}(q) \propto q^2$ at small q (see Eq. (37)). With ρ_p increasing, the dependence of $\hat{S}_{pp}(q)$ on q becomes weaker because of strengthening of intermolecular interactions. In this case we obtain a region of q, for which the power law $\hat{S}_{pp}(q) \propto q^{-x}$ is valid,

([2]) It should be noted that the static structure factor for monomers is sometimes defined as $\hat{S}(q) = 1 + \rho\hat{h}(q)/\hat{w}(q)$.

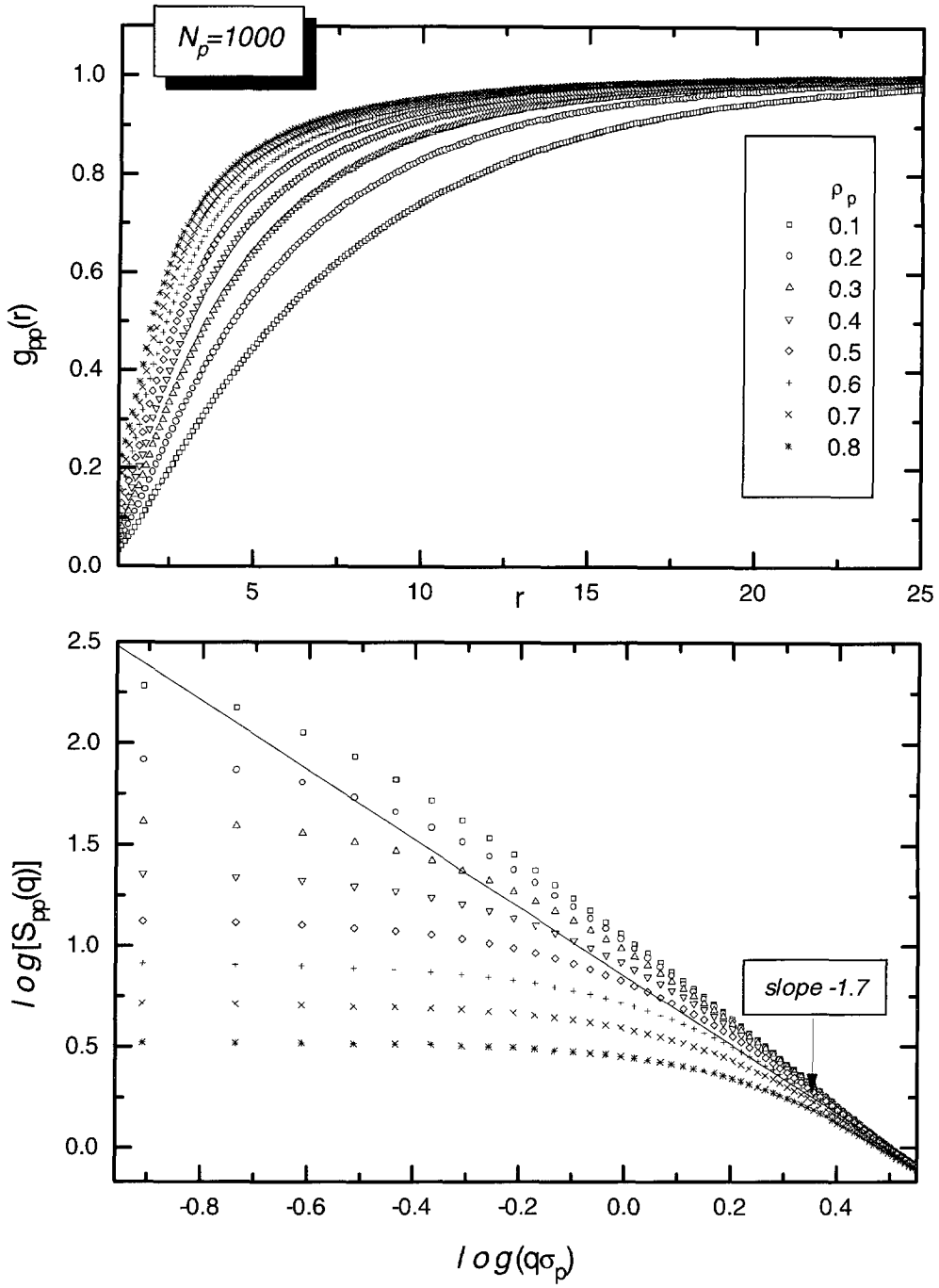

Fig. 3. — Correlation functions of a one-component system of chains of length $N_p = 1000$ at different density of segments ρ_p. Interaction of segments is described by the hard-sphere potential with $\sigma_p = 1$. Here and in other figures below the distance r is given in units of σ_p. For the structure factor presented in double-logarithmic coordinates the slope of the linear part of the curve is indicated, where $\hat{S}_{pp}(q) \propto q^{-1.7}$

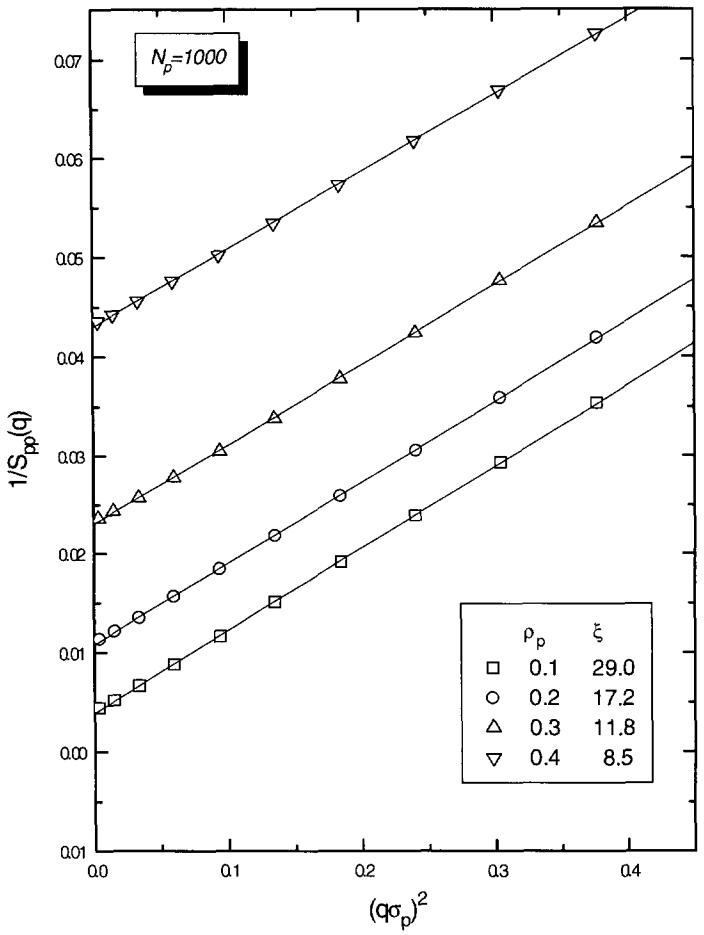

Fig. 4. — The Guinier dependence for the polymer structure factor of a one–component system of chains of length $N_p = 1000$ at different segment densities. Several values of the correlation radius ξ of density fluctuations are given (in units of σ_p). Interaction of segments is described by the hard–sphere potential with $\sigma_p = 1$. The lines connecting the calculated points are obtained by least squares fitting.

where x is close to 1.7. To evaluate the characteristic scale, *i.e.*, the radius of correlations of density fluctuations, ξ, we use the well–known relation [75,76]

$$\hat{S}(q) = \frac{k_B T \rho \chi_T \xi^{-2}}{q^2 + \xi^{-2}} \tag{38}$$

or $1/\hat{S}(q) = a + bq^2$, where $a = 1/\chi^*$ and $b = a\xi^2$. Figure 4 presents the examples of the dependencies of $1/\hat{S}_{pp}(q)$ on q^2 at small q (the so–called Guinier plot). In this figure we also indicate the values of ξ obtained for selected densities by least squares fitting of the linear parts of the curves. The calculations show that ξ is a decreasing function of ρ_p. In reference [69]. the correlation length ξ varied in the range 6–16.4 nm (depending on the concentration of the aqueous solution of PEO). This range corresponds to about 10 statistical segments of the chain. Our calculation gives a close or slightly smaller estimate for ξ in the region $0.3 \leq \rho_p \leq 0.8$ or $0.15 \lesssim \Phi_p \lesssim 0.4$.

4.2. HIGH–TEMPERATURE LIMIT. — For the binary system under consideration the simplest is the regime when no adsorption of chains occurs on the colloidal particles. This *athermal* regime corresponds to the condition $\epsilon_{dp} = 0$ or $T \to \infty$. Description of properties at such idealized conditions forms the basis for the following understanding of more complicated situations.

Figure 5 presents the correlation functions for the subsystem of colloidal particles at different number densities of the polymer component. As can be seen, the presence of even a small amount of polymer affects drastically spatial distribution of colloidal particles. Analysis of the function $g_{dd}(r)$ shows that with ρ_p increasing the main tendency is structurization of the colloid subsystem. The particles are pushed out of the regions occupied by chains, which results in growth of density fluctuations and increase of the contact values $g_{dd}(\sigma_d)$ at $r = \sigma_d$ and the values of $g_{dd}(r)$ at small interparticle distances. In the case $\rho_p \gtrsim 0.8$, even at the small density ρ_d considered here the colloidal particles start to form a *liquid–like* structure with the intensive first peak of the function $g_{dd}(r)$ and the secondary maximum at $r \approx 2\sigma_d$. At small q, the function $\hat{S}_{dd}(q)$ shows non–trivial behavior. As follows from Figure 5, the reduced compressibility, $\chi^* \equiv \hat{S}_{dd}(0)$, increases drastically with ρ_p from $\hat{S}_{dd}(0) < 1$ to $\hat{S}_{dd}(0) > 1$; however, with the following increase in ρ_p the function $\hat{S}_{dd}(0)$ decreases gradually. Figure 6 gives a good illustration of such a nonmonotonic dependence of the reduced compressibility. Note that the condition $\hat{S}_{dd}(0) = 1$ is fulfilled for the model under consideration at some threshold value $\rho_p \approx 0.015$.

The value of $\hat{S}_{dd}(0)$ is closely related to the characteristics of the effective (*i.e.*, mediated by the polymer medium) interparticle interaction. By analogy with definition of the second virial coefficient B (which characterizes the bare potential $u(r)$), let us write the expression for the *effective* virial coefficient:

$$B^* = 2\pi \int_0^\infty \left\{ 1 - \exp\left[-\frac{\psi(r)}{k_B T} \right] \right\} r^2 dr. \tag{39}$$

Here $\psi(r)$ is the potential of mean force, which is defined as

$$\psi(r) = -k_B T \ln[g(r)]. \tag{40}$$

From equations (39) and (40), we have

$$B^* = -2\pi \int_0^\infty h(r) r^2 dr = -\frac{1}{2}\hat{h}(0). \tag{41}$$

At $B^* > 0$ the repulsive interaction prevails under the given conditions; at $B^* < 0$ the effective attraction dominates: and at $B^* = 0$ (or $\hat{S}(0) = 1$) the balance of the attractive and repulsive forces is established (*i.e.*, this is an *isopoint*) and the system behaves as a *quasiideal* one. Let us clarify the term "quasiideality". For an ideal system of noninteracting nonbonded particles we have: $\hat{S}(q) = 1$ at any q. In the presence of interactions, heterogeneities (at least local) of density distribution always exist. In this case the system can be considered as a *quasiideal* one if under the given conditions its large–scale properties (in particular, compressibility) coincide with similar characteristics of the reference ideal system.

As follows from Figure 6, in the athermal regime there is a considerable effective attraction between the particles in a wide range of ρ_p. Such a behavior is due to steric (*i.e.*, entropic) factors only. A detailed qualitative analysis of the observed effects is given by de Gennes for a lattice model [4]. According to reference [4], in the limit of large ρ_p at $\rho_d \to 0$ and $N_p \to \infty$ we must have: $B^*_{dd} \to 0$ or $\hat{S}_{dd}(0) \to 1$. This is explained by a complete screening of the bare

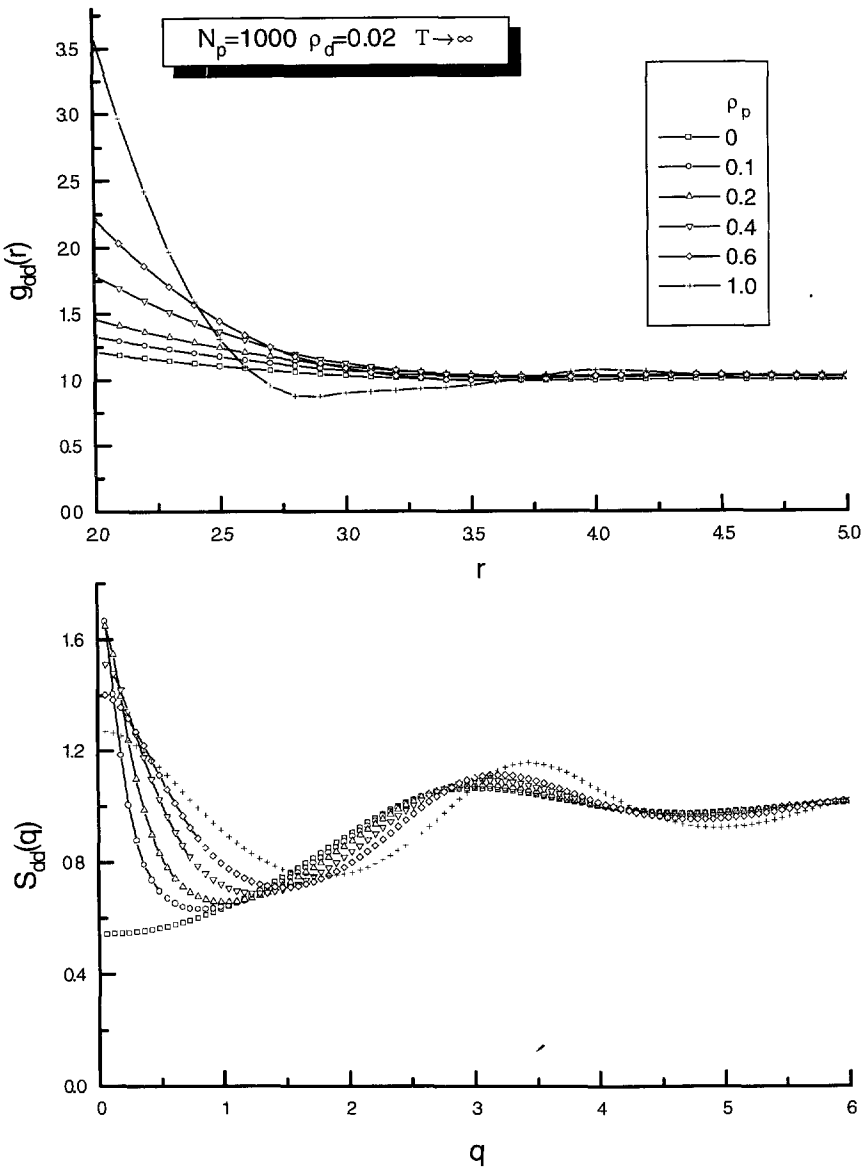

Fig. 5. — Correlation functions for a subsystem of colloidal particles in the binary system of the particles and polymer chains at different densities of polymer segments. The calculations correspond to the high–temperature limit. All interactions in the system are described by the hard–sphere potential. Particle density is $\rho_d = 0.02$. Chain length is $N_p = 1000$.

potential u_{dd} by long polymer chains in an extremely dense (incompressible and defect–free) polymer matrix. Our results shown in Figure 6 confirm this conclusion. Really, at large ρ_p there is a well–pronounced tendency for $\hat{S}_{dd}(0)$ to approach 1, *i.e.*, the transition to the quasiideal conditions is observed. Note that for the system studied the quasiideal conditions are realized in two cases: at low values of ρ_p and in the limit of large ρ_p. In the following discussion we will use the superscript "o" to identify the values of the parameters at the isopoint.

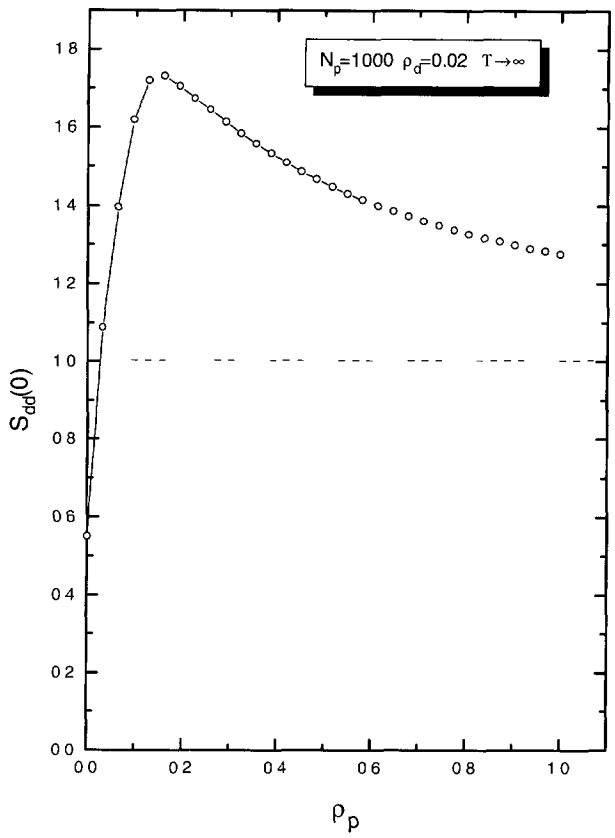

Fig. 6. — Reduced isothermal compressibility $\chi^* \equiv \hat{S}_{\mathrm{dd}}(0)$ of the subsystem of colloidal particles as a function of segment density. The calculations correspond to the high-temperature limit. All interactions in the system are described by the hard-sphere potential. Particle density is $\rho_{\mathrm{d}} = 0.02$. Chain length is $N_{\mathrm{p}} = 1000$.

4.3. WEAK ADSORPTION. — At fixed value of the parameter $\epsilon_{\mathrm{dp}} = -1$ the intensity of adsorption is regulated by temperature ([3]). Figures 7 and 8 give examples of calculated pair correlation functions $g_{\mathrm{ij}}(r)$. where i, j = d, p. As can be seen from Figure 7, with temperature T decreasing (*i.e.*, adsorption increasing) the function $g_{\mathrm{dd}}(r)$ diminishes in the region of small interparticle distances r and simultaneously begins to grow at $r \approx 3.5$ forming a distinct maximum at this point. We can say that decrease in T results in the transfer of the first high-temperature maximum to the second peak lying at larger distances. Such behavior indicates that when adsorptional sticking to chains occurs the particles draw apart and the corresponding distances redistribute in space so that the optimum environment of the particles arranged by the redistribution of a polymer component is achieved.

The function $g_{\mathrm{dp}}(r)$ takes its maximum value in the region of the potential well ($1.5 < r < 2$). where it is nearly constant. and quickly increases in this interval of r with T decreasing. The origin of the second maximum of $g_{\mathrm{dp}}(r)$ at $r \approx 2.5$ can be explained by the fact that a segment sticked to the surface of a colloidal particle attracts the neighboring segment of the same chain

([3]) The temperature, T, is measured in units of $k_{\mathrm{B}}T/|\epsilon_{\mathrm{dp}}|$.

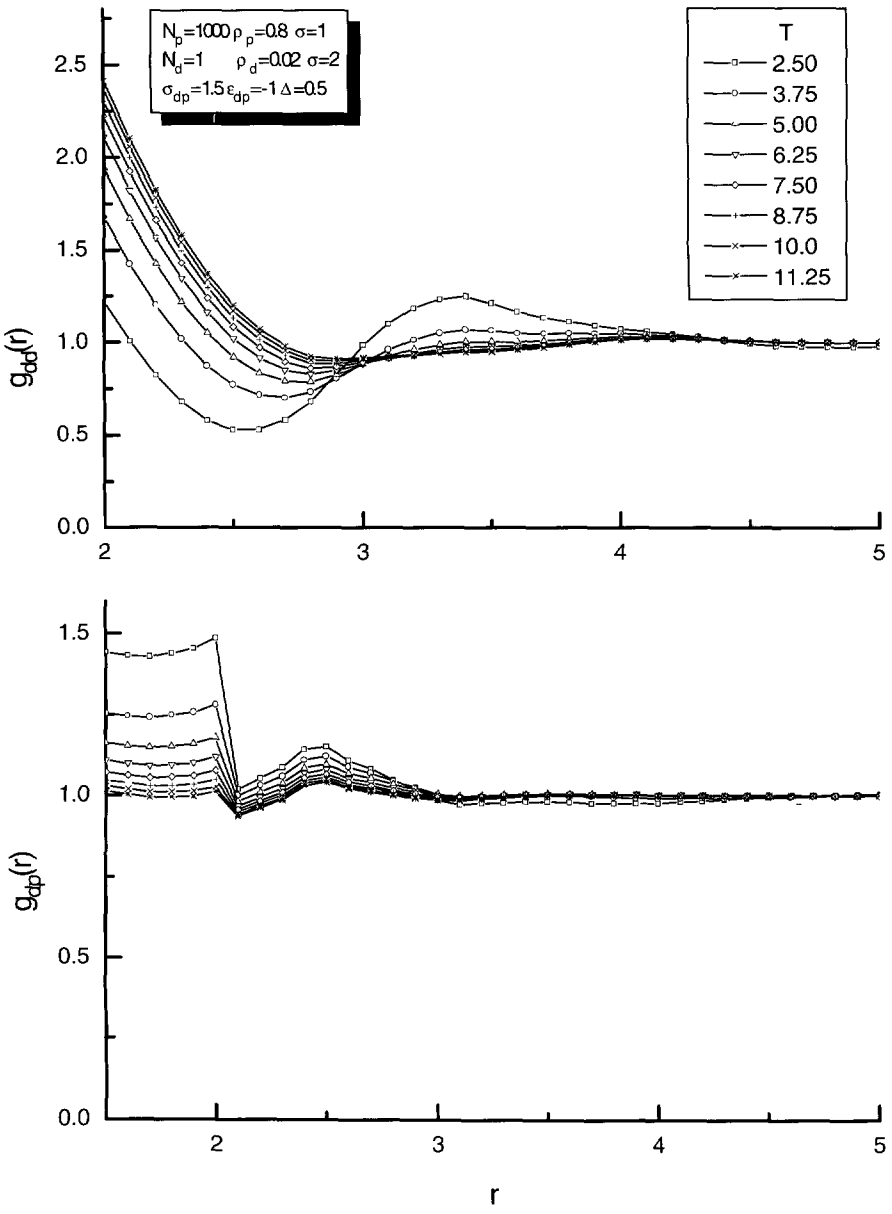

Fig. 7. — Particle–particle (dd) and particle–polymer (dp) pair correlation functions calculated at different temperatures with adsorption interaction taken into account. Particle and segment densities are 0.02 and 0.8, respectively. Chain length is $N_p = 1000$.

(the sum of the corresponding distances is $r = \sigma_d/2 + \sigma_p/2 + l = 2.5$).

With ρ_p increasing, at constant temperature and density ρ_d the function $g_{dd}(r)$ undergoes the evolution (see Fig. 8) that reminds the temperature changes (see Fig. 7). At the same time, the correlation function $g_{pp}(r)$ does not exhibit any qualitatively new properties.

Let us now consider the temperature dependence of $\hat{S}_{ij}(0)$ and B^*_{ij} (i,j = d,p). Figures 9 and 10 give some typical examples of these dependencies. As can be seen, in both cases the

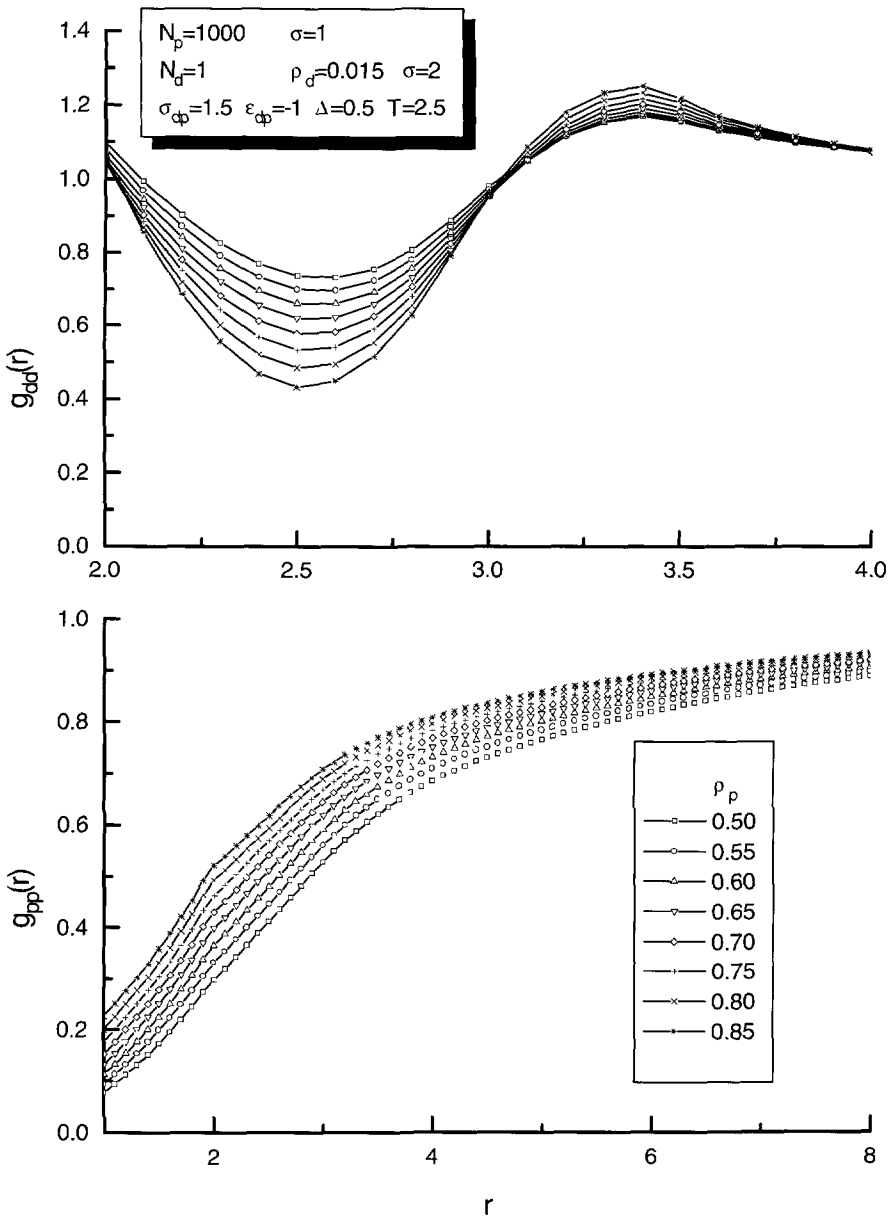

Fig. 8. — Particle–particle (dd) and polymer–polymer (pp) pair correlation functions at $T = 2.5$ and various densities of polymer segments with adsorption interaction taken into account Particle density is $\rho_{\rm d} = 0.015$. Chain length is $N_{\rm p} = 1000$. The function $g_{\rm pp}(r)$ has a weakly pronounced break at $r = 2\sigma_{\rm p}$, which is due to the intramolecular structure of the chain.

behavior of the functions of the dd and pp types is nonmonotonic: there is a slow decrease (increase) at high T and a sharp growth (drop) at low T. On the other hand, with decrease in temperature the effective virial coefficient $B^*_{\rm dp}$ always decreases showing rather quick transition from positive to negative values. This indicates strengthening of the adsorption effects. In the

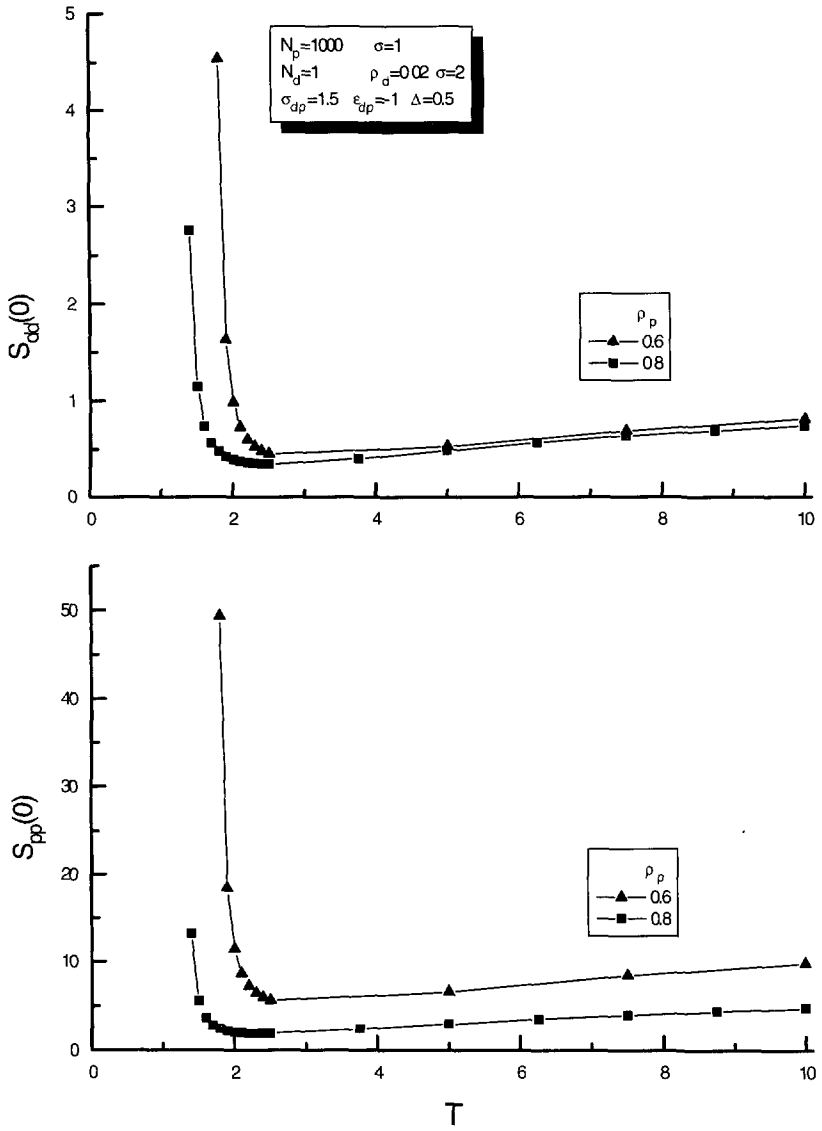

Fig. 9. — Temperature dependencies of reduced isothermal compressibility for the colloidal and polymer components at two segment densities. Density of colloidal particles is $\rho_d = 0.02$. Chain length is $N_p = 1000$.

considered range of T the function B^*_{pp} always remains positive. Therefore, the spatial density distribution of the polymer component does not undergo any considerable (qualitative) changes at weak (or moderate) adsorption. although certain structural changes surely occur.

The functions $\hat{S}_{dd}(0)$ and B^*_{dd} exhibit the most interesting behavior. At a given density ρ_p, there are two temperatures T^o corresponding to an isopoint. In other words, for the colloidal component the above-mentioned condition of quasiideality ($\hat{S}_{dd}(0) = 1$ or $B^*_{dd} = 0$) is achieved twice: at relatively high temperature $T = T^o_1$ and at lower temperature $T = T^o_2$. Figure 11a

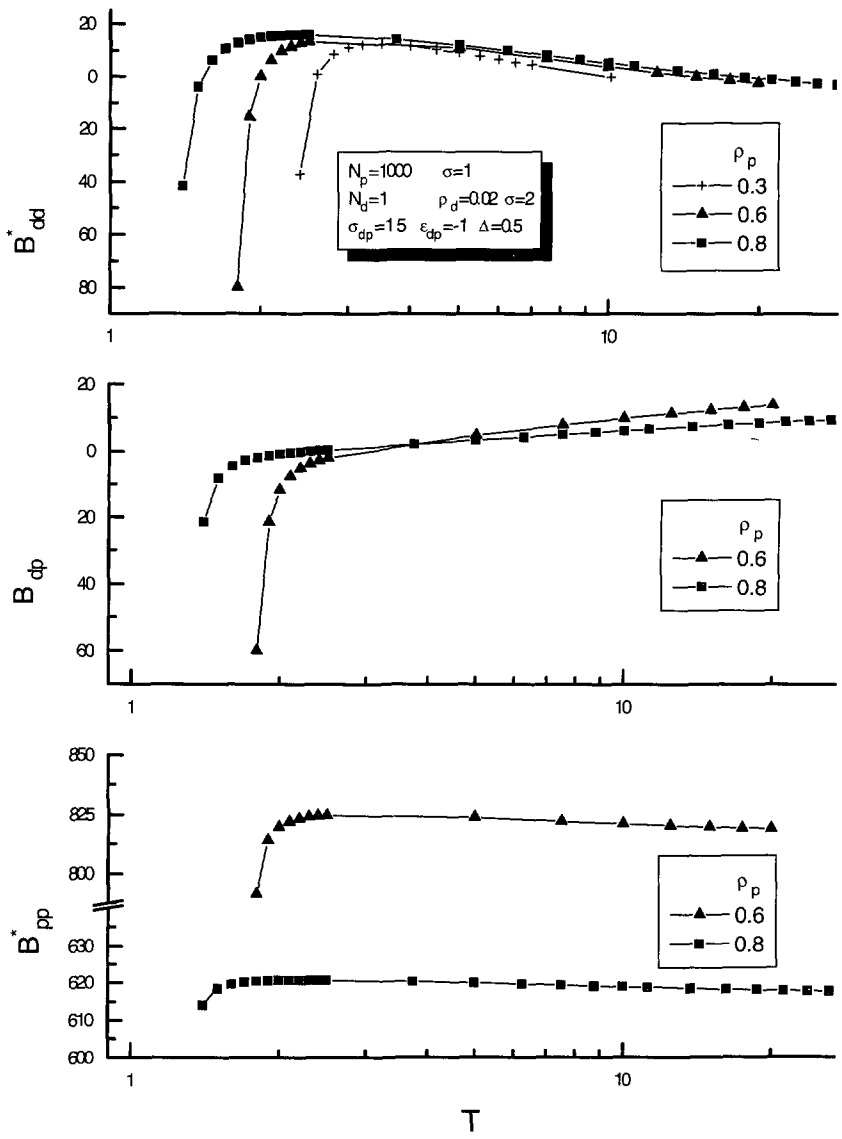

Fig. 10. — Temperature dependencies of B^*_{ij} (i, j = d, p) for various densities of the polymer component at particle density $\rho_d = 0.02$ and chain length $N_p = 1000$. For better visualization the logarithmic scale is used for temperature.

presents the results of the detailed calculation, given in double–logarithmic coordinates for better visualization. The curves of Figure 11a (the upper one (1) and the lower one (2)) define the pairs of values T_1^o, ρ_p^o or T_2^o, ρ_p^o, respectively, *i.e.*, these curves describe the *upper* and *lower* isopoints.

At temperatures between curves 1 and 2, there is a wide region, A, characterized by small compressibility of the subsystem of colloidal particles ($\hat{S}_{dd}(0) < 1$). In this region, the repulsive forces prevail in the effective interaction of the particles. We can call this region "*the region*

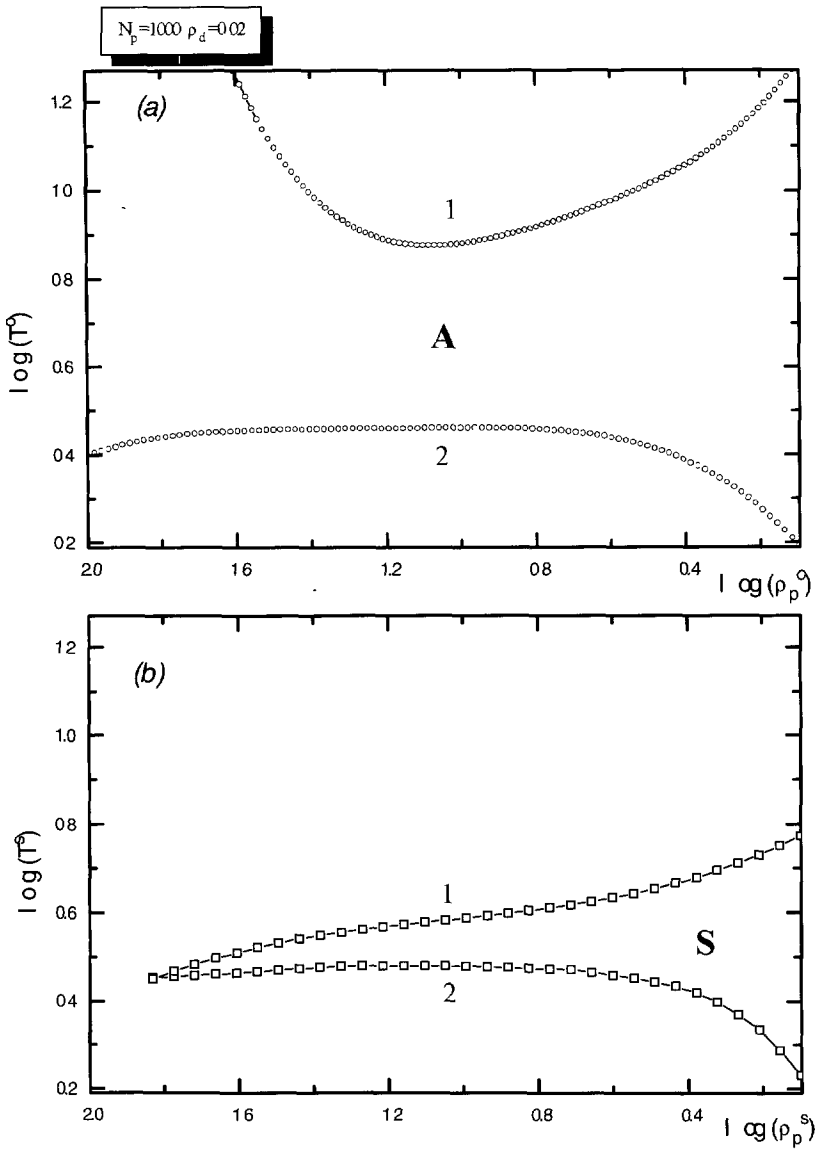

Fig. 11. — Temperature–concentration state diagrams for the colloidal component in the regime of weak (moderate) adsorption. (a) The curves of quasiideal behavior. In the region A the partial compressibility is $\chi^* < 1$; above curve 1 and below curve 2, $\chi^* > 1$. (b) The subregion S of the increased stability of the colloidal component. On the boundaries of this subregion (curves 1 and 2) χ^* is the same as for a one–component system of particles. Particle density is $\rho_d = 0.02$; chain length $N_p = 1000$. At $\rho_p < 0.05$ and $\rho_p > 0.8$ the dependencies were not calculated.

of stable states". At high densities ρ_p, *i.e.*, in the case of polymer melt, the region A infinitely expands up to $T = T_1^o \to \infty$ and spreads down to the point $T = T_2^o \to 0$. At low densities ρ_p, the situation is different. At ρ_p less than some threshold value $\rho_p = \rho_p^{(1)}$ ($\rho_p^{(1)} \approx 0.015$ at $\rho_p = 0.02$) an unlimited expansion of the region of stable states is observed. Note that

the threshold value $\rho_p^{(1)}$ does not depend on the particle density ρ_p in the system. In the lower part of the diagram shown in Figure 11a there must be also a threshold value $\rho_p = \rho_p^{(2)}$ corresponding to $T_2^o \to 0$. We can say that $\rho_p^{(2)} < \rho_p^{(1)}$ at finite ρ_d. Although the detailed analysis of the limiting case $\rho_d \to 0$ is possible within the framework of the RISM theory [51], we will not consider the corresponding questions in this paper.

In addition to the region A, we have in the diagram of states of Figure 11a two more regions corresponding to temperatures above curve 1 or below curve 2. In these regions, compressibility of the system is more than unity and, therefore, is considerably higher than in the absence of polymer additives. In these regions, B_{dd}^* is negative, *i.e.*, under these conditions the addition of a polymer results in the effective mutual attraction of the colloidal particles. Therefore, in the binary system the particles show a tendency to aggregation.

It is necessary to note the following two circumstances related to the problem of aggregation stability. First, the characteristics discussed here give only an indirect information about aggregation of the particles and reveal only general tendencies of this process. For a more complete description, the direct calculation of average aggregate sizes is necessary. Second, at the conditions under consideration, the binary system always remains a single–phase one, *i.e.*, it is stable at macroscopic scale. In other words, there is no large–scale inhomogeneities of the component distribution in the system. However, as is shown in the following subsections, the situations with large–scale fluctuations of density of the colloidal particles or with the formation of partially ordered quasiregular structure are possible as well.

Inside the region of stable states A we can locate a special subregion of "*absolute stability*" (the subregion S in Fig. 11b), where compressibility of the colloidal component is lower than the one observed at the same value of ρ_d for the system of individual particles (*i.e.*, without polymer additives). An indication to the existence of such states follows, in particular, from comparison of the values of $\hat{S}_{dd}(0)$ at the minimum of the temperature dependence (see Fig. 9) and the values of $\hat{S}_{dd}(q)$ characterizing the individual component at $q \sim 0$ (see Fig. 2). Two temperatures (the upper $T = T_1^S$ and the lower $T = T_2^S$) correspond to each density $\rho_p = \rho_d^S$ belonging to the subregion S. The pairs of values T_1^S, ρ_p^S and T_2^S, ρ_p^S define the two curves (the upper one (1) and the lower one (2)) that are the boundaries of the subregion S of the state diagram (see Fig. 11b). On the boundaries of the subregion S compressibility of the subsystem of colloidal particles coincides with compressibility of the pure colloid system; inside the subregion S the compressibility is lower. This region of the parameters T and ρ_p lies close to the lower curve of the quasiideal behavior (curve 2 of Fig. 11a). One can say that, in the case of weak (or moderate) adsorption, the polymer additives increase the aggregation stability in the subregion S, *i.e.*, the polymer plays the role of a stabilizer of the dispersion. The detailed discussion of the problems connected with the stabilizing action of macromolecules is the subject of a special publication.

4.4. Strong Adsorption. — At low temperatures belonging to the region of $T < T_2^o$ considerable structural changes occur. The correlation functions $g(r)$ presented in Figures 12 and 13 indicate these changes. The example given in Figure 12 shows that the function $g_{dd}(r)$ is characterized by qualitatively new features, as compared to the case of weak adsorption (see Fig. 7). The main peculiarity is the appearance of the regime typical for the system in the vicinity of critical conditions. In this regime we observe not usual quickly damped oscillations but long tails of the function $g_{dd}(r)$. At large r, the asymptotic decrease of these tails can be described by the Ornstein–Zernike relation [75, 106]

$$g(r) - 1 \propto \frac{1}{r} \, e^{-r/\xi}, \tag{42}$$

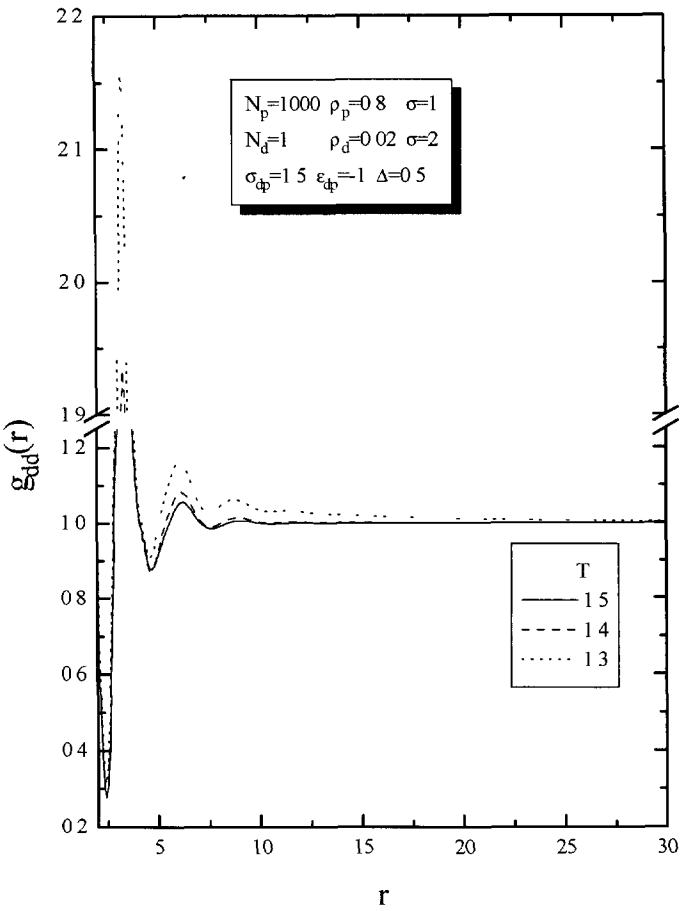

Fig. 12. — Pair correlation function of the subsystem of colloidal particles in the regime of strong adsorption of macromolecules at three different temperatures. The particle and segment densities are 0.02 and 0.8, respectively; $N_p = 1000$. Note the presence of long tails of the correlation function and its specific features at small distances.

which is directly associated with equation (38). The fact that the long–range correlations of the characteristic scale $\xi \sim 10$ are present in the system indicates a direct analogy with the critical behavior (the process of colloidal aggregation or "condensation").

The nontrivial changes in the density distribution of polymer segments should be mentioned as well. If density ρ_p is not too high, then at sufficiently low temperatures the pair correlation function $g_{pp}(r)$ differs drastically from the typical one for a system of chains in a good solvent (*i.e.*, in the case when the repulsive forces between the segments prevail). As follows from the example presented in Figure 13, in a narrow temperature interval the pair correlation function $g_{pp}(r)$ changes its behavior from the curve increasing monotonically from $g_{pp}(\sigma_p)$ to 1 to the curve with a maximum and a long tail slowly decreasing to 1. Note that such a transition is observed only at sufficiently low concentrations of the polymer.

Now let us consider behavior of the $\hat{S}_{dd}(q)$ function in the region of strong adsorption. It is well-known that the scattering at the low q limit diverges not only at the critical point but also at each point of the spinodal curve. At ρ_d = const. the particular conditions for the

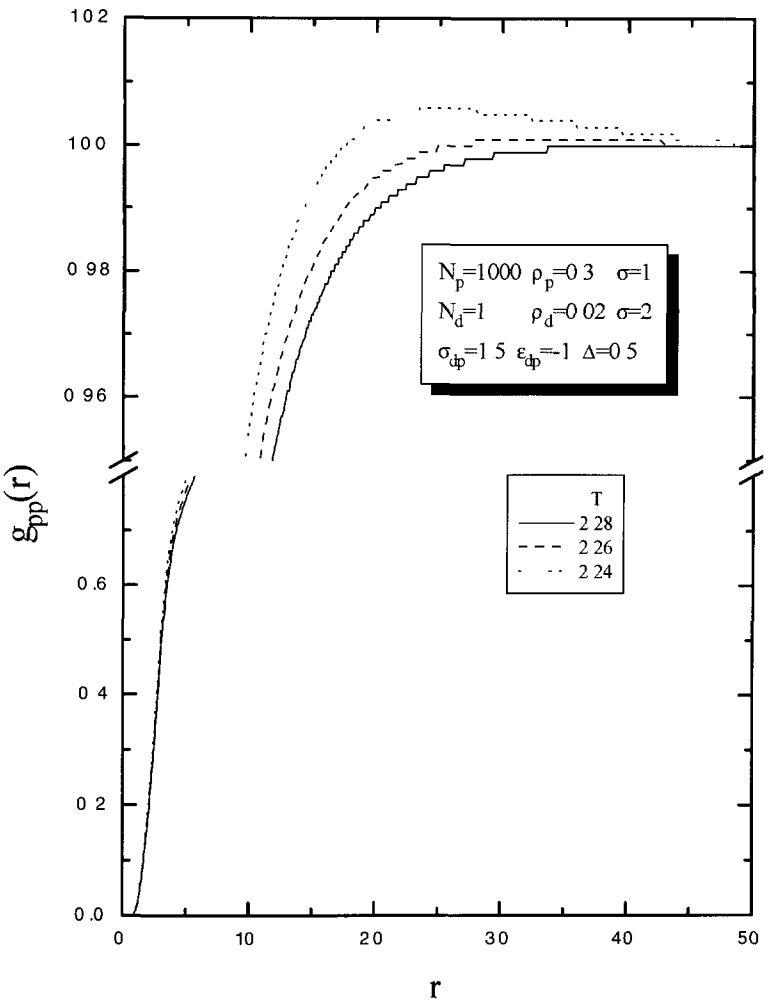

Fig. 13. — Pair correlation function of the polymer subsystem in the regime of strong adsorption at three different temperatures. The particle and segment densities are 0.02 and 0.3, respectively; $N_p = 1000$. At $T \leq 2.24$ the correlation function shows an abnormal behavior in the region of $r \approx 20$. Under these conditions, the effective attraction of segments prevails ($B^*_{pp} < 0$), *i.e.*, the chains are found in a thermodynamically poor solvent.

colloidal component are achieved at some values of the parameters $T = T^*$ and $\rho_p = \rho_p^*$, which define the spinodal line of a phase separation. At these points we must have a singularity in compressibility χ_T of the given subsystem. We have already noted quick increase of the reduced compressibility $\hat{S}_{dd}(0)$ when crossing the lower curve of quasiideality (see Fig. 9). Now it is necessary to perform calculations at lower temperatures, for which $\hat{S}_{dd}(0) \to \infty$. Unfortunately, it is rather difficult to solve the integral equations in the vicinity of T^*. Therefore, we used extrapolation to the limiting case $1/\hat{S}_{dd}(0) \to 0$. Figure 14 presents the results of calculations for some values of ρ_p. As can be seen, at $\rho_p \gtrsim 0.6$ the points calculated for our model fall on a straight line in the coordinates $1/\hat{S}_{dd}(0) - T$. This fact provides reliable estimates for T^*. However, at lower ρ_p deviations from the straight line occur and the estimates of T^* were

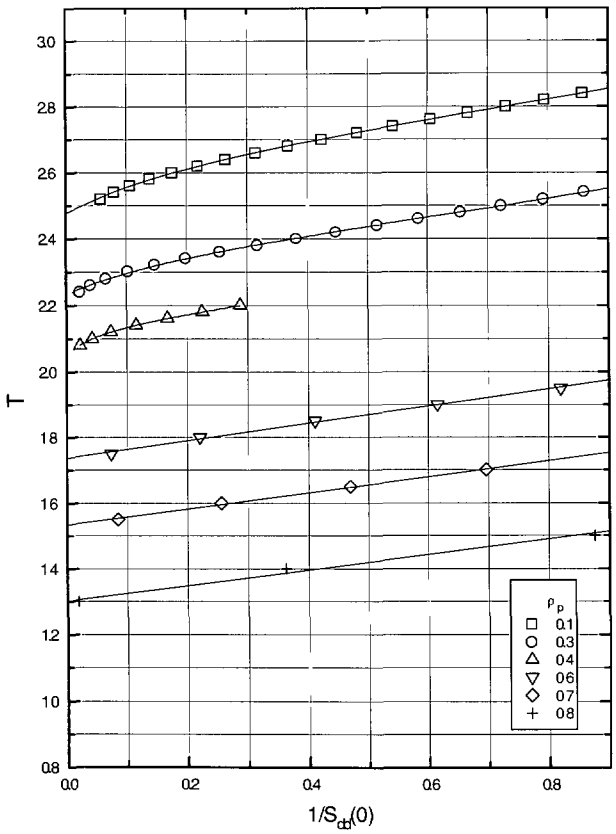

Fig. 14. — Determination of the temperature T^* of the colloidal component at different polymer densities in the regime of strong adsorption by extrapolation of the dependencies presented. The value of T^* corresponds to the condition $\hat{S}_{dd}(0) \to \infty$. The particle density is $\rho_d = 0.02$; chain length, $N_p = 1000$.

obtained using more complex regression equations, and are less reliable. At $\rho_p < 0.08$ we failed to find an estimate for T^*. Figure 15 presents the temperatures T^* plotted against the corresponding densities ρ_p^*. For better visualization we use double–logarithmic coordinates. The line passing through the calculated points is the spinodal curve of the state diagram of the subsystem of the colloidal particles. At temperatures above the spinodal curve, the volume distribution of particles is rather uniform. At $T < T^*$ condensation of particles occurs. This process must be accompanied by appearance of large aggregates ("drops" of the liquid phase). In the vicinity of the spinodal curve the liquid–like and gas–like phases coexist with each other.

We failed to calculate the spinodal curve in the region of very small polymer concentrations. However, one can assume that the temperature T^* must decrease monotonically with the decrease of the polymer content in the system. Really, for the same effect to be achieved the loss in the number of adsorption contacts (which causes condensation) in the region of small ρ_p can be compensated only by the increase in intensity of contacts. In addition to this, it is evident that $T^* \to 0$ at $\rho_p \to 0$; this means that at infinitely small polymer concentration infinitely large influence on the particles is necessary to achieve any effect. Note also that T^* must drop to zero in the limit of large ρ_p at $N_p \to \infty$.

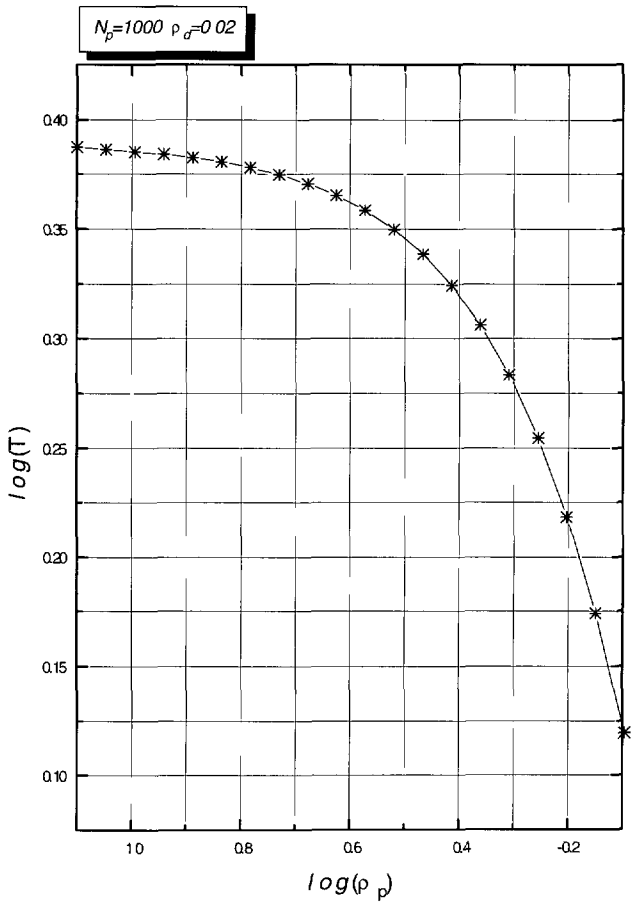

Fig. 15. — The temperature–concentration diagram of states of the subsystem of colloidal particles. The spinodal curve corresponds to $\hat{S}_{dd}(0) \to \infty$. The particle density is $\rho_d = 0.02$; chain length, $N_p = 1000$. At $\rho_p < 0.08$ and $\rho_p > 0.8$ calculations were not performed.

4.5. AGGREGATION MECHANISM. — A considerable body of literature exists relating to the interaction of polymers with a flat infinite surface and the interaction between solid surfaces in the presence of polymer solution (see, *e.g.*, Refs. [1, 13, 18. 20, 37–49, 107]). It has been shown that in an athermal system at $\rho_p \ll 1$ and $\sigma_d/\sigma_p \to \infty$ the resulting osmotic pressure $\Delta\Pi$ (which is the difference of the pressure in the gap between the two surfaces and the pressure on the external surfaces) has the asymptotic: $\Delta\Pi \to +0$ at $r_{dd} \to \infty$ and $\Delta\Pi \to -k_B T\rho_p/N_p$ at $r_{dd} \to 0$, where r_{dd} is the distance between the two surfaces. As a result, we have at small r_{dd}: $\Delta\Pi < 0$, *i.e.*, under the external pressure the particles stick together. In other words, the polymer mediated surface–surface interaction is attractive. This "steric" aggregation mechanism is universal, *i.e.* valid both for high and low temperatures, as well as for infinite surfaces and for small colloidal particles. The physical reason is that the polymer chains are ousted from the gap between the particles creating the osmotic pressure difference between this gap and external solution. In the last case, however, the aggregation tendency is weak and does not lead to phase separation. Note that at large $\rho_p \sim 1$, when the

solvent (or free volume) is absent in the system, approach of the surfaces (or particles) to each other gives no gain in free energy.

Adsorption can have a considerable effect as well [15, 25, 45, 107]. At strong adsorption, the energy contribution has a dominant role, because the chain fragments found in the gap between the two surfaces (or colloidal particles) play the role of bridges. If the characteristic sizes σ_d and σ_p are comparable then the role of this energy contribution becomes less important. However, at low temperatures it is the main reason of intensive aggregation of particles. In addition, one could mention another mechanism of aggregation, where particles with saturated adsorption layers would be connected to each other through excess particles. This mechanism has been discussed by Alexander [15] in the context of polymer adsorption onto micelles.

Thus, in the case of strong adsorption the theory predicts that the polymer additives cause sharp strengthening of aggregation processes. In a real system this must result in flocculation. *i.e.*, in the appearance of macroscopic regions rich in colloidal particles. Under such conditions each particle is covered with a dense polymer laver and bridging fragments of chains provide sticking of separate particles to each other.

4.6. Ordered Structures. — As is mentioned above, the first maximum of the structure factor $\hat{S}_{dd}(q)$ (see Figs. 2 and 5) characterizes usual (statistical) order arising from almost random collisions of particles. This behavior is typical for a wide region of parameters. However, it turns out that the conditions are possible, under which both components form well–ordered quasiregular structures, the scattering functions of which are characterized by some special features.

Let us follow the temperature evolution of the structure factors presented in Figure 16. At high temperatures these functions exhibit an ordinary behavior. However, if the temperature becomes sufficiently low, then a new maximum appears in the structure–factor curves of both components at certain $q = q^+$. Note that for the subsystem of colloidal particles the value of q^+ is considerably smaller than the value of q_1 that characterizes the position of the main peak for the individual component or for the binary system at high temperatures. For the polymer, the peak at q^+ appears first at smaller q than for the colloidal particles. but with further decrease of temperature it shifts to the right.

The calculation shows that the appearance of the q^+ peak in a structure–factor curve of the polymer component is possible only at sufficiently high densities of the two components. Figures 17 and 18 give an illustration to this statement. For the colloidal particles, the effect discussed is observed in a somewhat larger range of densities. In this case. the value of q^+ depends on ρ_d (it shifts to the right with ρ_d increasing) but almost does not depend at all on ρ_p. On the other hand, for a polymer component the growth in ρ_p results in q^+ shifting to larger q. Note also that appearance of the q^+ peak for the colloidal particles is accompanied by disappearance of the initial q_1 peak. At last, note that under the same conditions the position of the polymer q^+ peak does not vary with the chain length N_p (at $N_p \gtrsim 10^2$).

Figure 19 presents the temperature T^+ of appearance of the polymer q^+ peak plotted against the corresponding density $\rho_p = \rho_p^+$. The curve in Figure 19 must be considered as the curve of the state diagram: the states with periodic (quasiregular) structures are realized below this curve. Note also that this curve starts in the vicinity of the curve of critical states of the system.

Therefore, the results presented above indicate considerable structural changes due to the formation of specific states characterized by binding together chains and particles. The peak of the polymer structure factor at $q \neq 0$ indicates the presence of large fluctuations of density. This means that alternating regions with lowered and elevated segment densities are formed in the system. This structure exhibits a set of interesting properties, *e.g.*, very low compressibility.

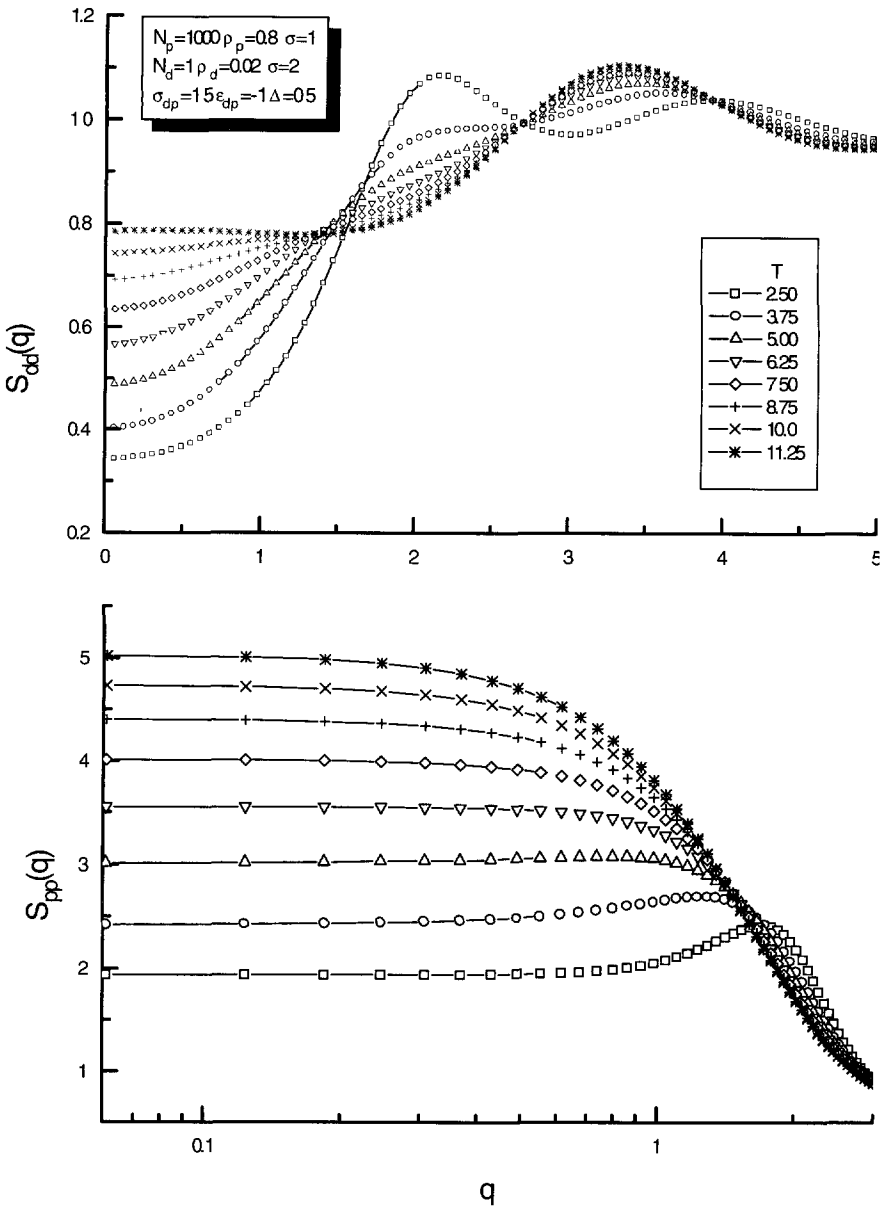

Fig. 16. — Partial structure factors for the colloid and polymer subsystems at different temperatures. The particle and segment densities are 0.02 and 0.08, respectively; $N_p = 1000$. In the case of the polymer subsystem the logarithmic scale is used for q.

Let us try to explain the observed effects.

When adsorption is strengthened, an adsorption layer of polymer segments is formed. Figure 7 illustrates this process. In the case of the short–range adsorption potential used in this study, the adsorption layer as a whole consists of a layer of polymer segments within the adsorption potential well (with the width of order of the width of a monolayer) and a somewhat more expanded "corona". Due to the presence of the corona, the local segment

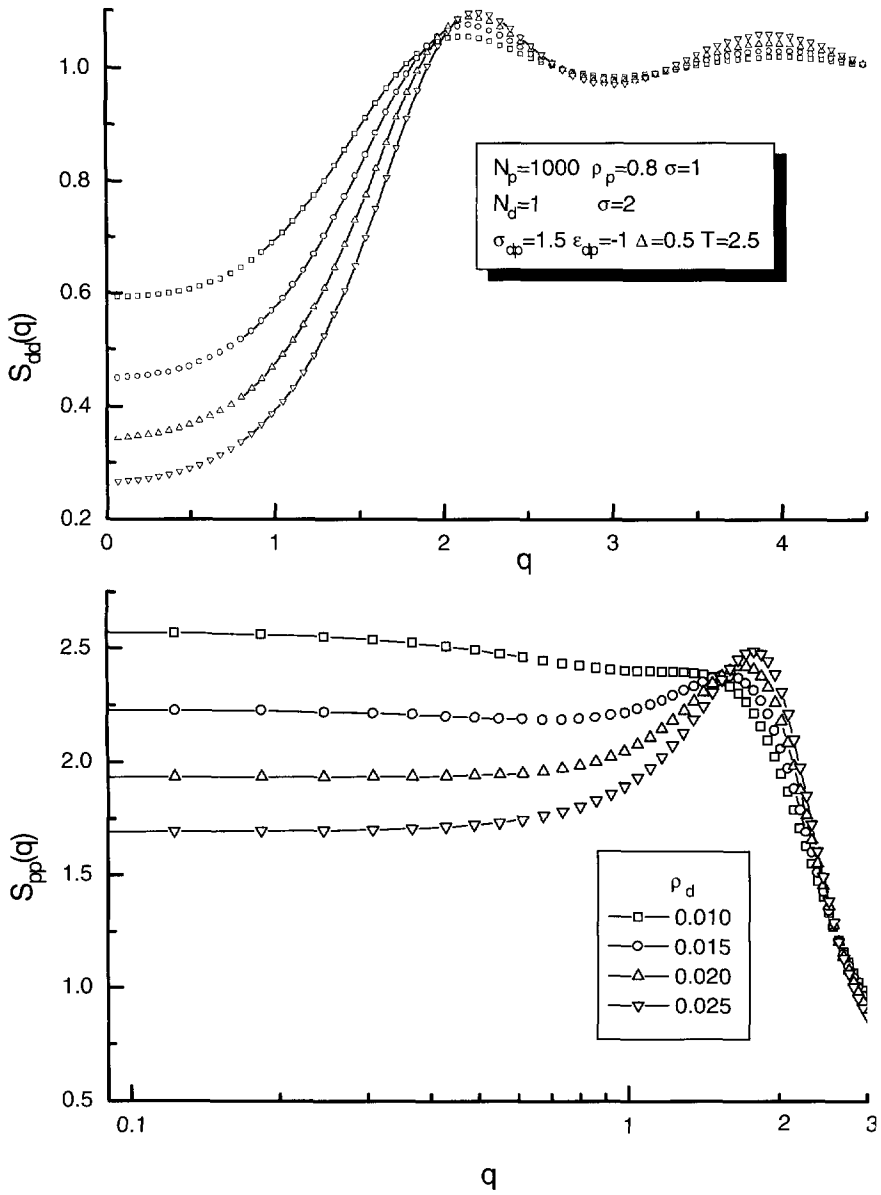

Fig. 17. — Partial structure factors for the colloid and polymer subsystems at $T = 2.5$ and different particle densities. The segment density is 0.8; $N_p = 1000$. In the case of the polymer subsystem the logarithmic scale is used for q.

density just outside the adsorbed monolayer is somewhat higher than the average (over the whole system) value of ρ_p and decreases rapidly in the radial direction. A colloidal particle together with the neighboring polymer–rich shell can be considered as a single adsorption complex (the $\mathcal{A}$ complex). From this point of view, to describe the structure of the system under the conditions discussed, one should consider interaction and spatial distribution of these $\mathcal{A}$ complexes. A specific feature of interaction of such subunits is that the corresponding effective

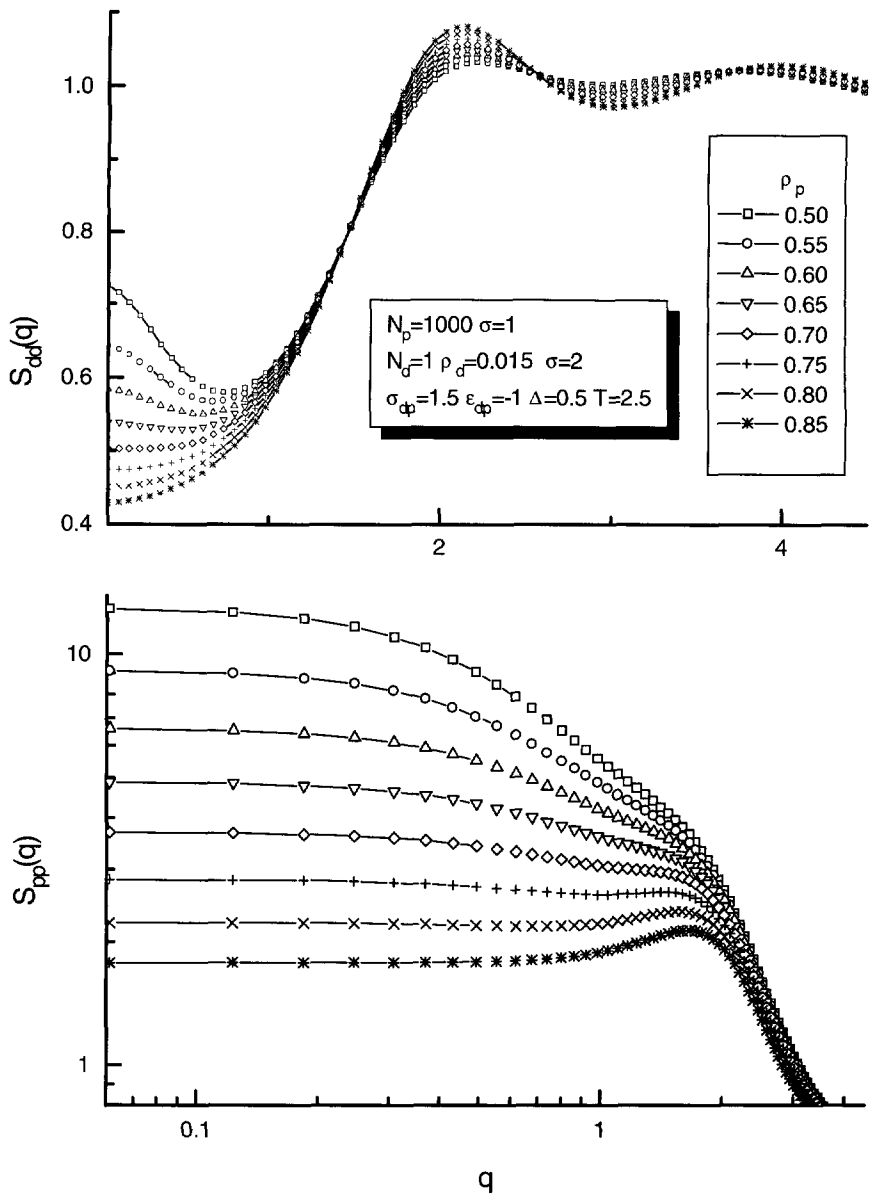

Fig. 18. — Partial structure factors of the colloid and polymer subsystems at $T = 2.5$ and different segment densities. The particle density is 0.015; $N_p = 1000$. In the case of the polymer subsystem the logarithmic scale is used for q.

potential $\psi_A(r)$ consists of two parts: the internal hard core of diameter $\sigma_A \approx \sigma_d + \sigma_p$ and the subsequent "soft" screening part, where $\psi_A(r)$ diminishes rather quickly with the increase of r. It is evident that in the case of adsorption of small molecules on particles the screening tail of the potential $\psi_A(r)$ is absent. The presence of this tail is characteristic only for a polymer–containing system. Packing of the $\mathcal{A}$ complexes with the interaction potential of this type may result in the formation of quasiregular arrays, in which the $\mathcal{A}$ complexes move

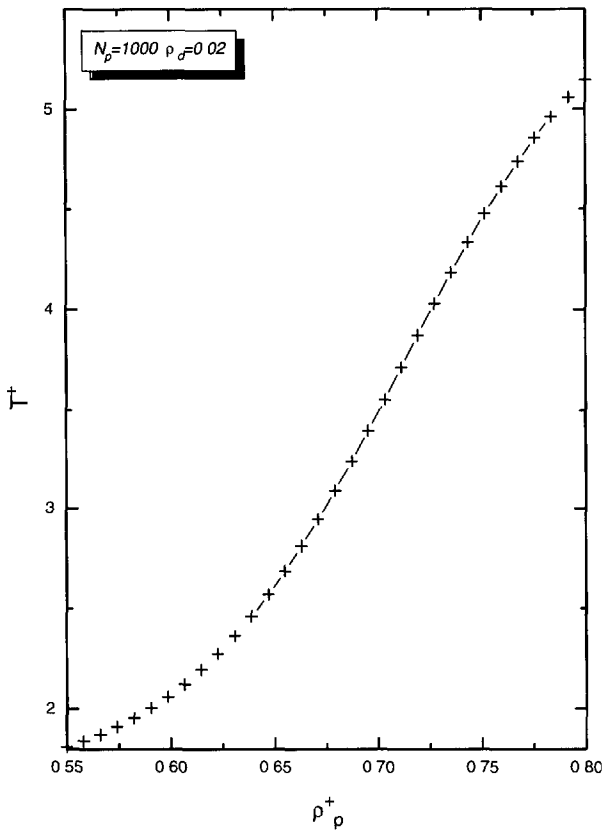

Fig. 19. — The temperature–concentration diagram describing the conditions, under which periodic (quasiregular) structures are formed. Such states are realized below the curve connecting the calculated points. The particle density is 0.02; $N_p = 1000$.

freely but at the same time the average positions of their centers correspond to some sites of a regular quasilattice (*cf.* Wigner crystals, see Refs. [108, 109]). Naturally, this must lead to a considerable nonuniformity in distribution of both colloidal particles and polymer segments. This nonuniformity of density distribution manifests itself as appearance of the q^+ peak of structure factors.

Figure 20 gives an attempt to represent the distribution of density of polymer segments under the conditions described above. In positioning spherical structural subunits (*i.e.*, $\mathcal{A}$ complexes) in space we took into account only the elements of symmetry corresponding to a simple cubic lattice. For more complex lattices additional peaks of structure factors would appear, which is not observed in our study and in the experiment [69] (see below). The periodic structure presented in Figure 20 is similar to the Schwarz surface [110, 111], which is topologically equivalent to a simple cubic lattice. The lattice sites (cavities in Fig. 20) are occupied by the colloidal particles. Near the cavities (*i.e.*, particles) the segment density is maximal. Each site is linked with six nearest neighbors by channels, in the central part of which the segment density is minimal. Position of the q^+ peak defines the period of the structure r^+ ($r^+ = 2\pi/q^+$). Apparently, here we have in mind only average periodicity; heat motion destructs the regular structure and provides a nonzero probability of direct contacts between the particles. Note that nearly all the states corresponding to a quasiperiodic structure belong

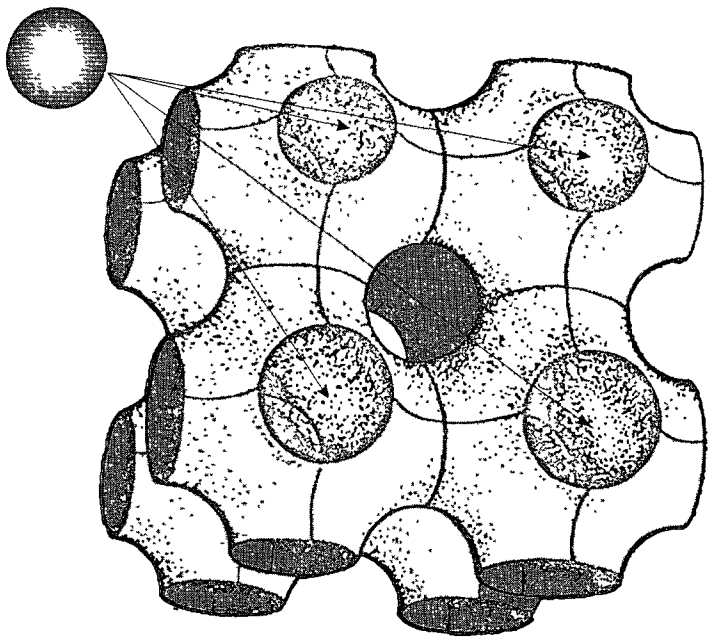

Fig. 20. — The schematic representation of density distribution of polymer chains in a system of colloidal particles and polymer chains, in which a quasiperiodic structure of adsorption complexes is formed. Continual representation of the distribution of segments is used. The representation is constructed by analogy with the Schwarz surface [110]. The cavities of the structure are occupied by colloidal particles.

to the subregion of the "increased" stability (*i.e.*, the region S in Fig. 11b). We recall that a very low compressibility of the system is typical for this subregion. In the next section we compare some of the above-mentioned results of calculation with the experimental data.

4.7. Comparison with the Experiment. — As is shown in reference [69], binding of micelles with PEO macromolecules in a semidilute solution results in a considerable change of properties of both subsystems, as compared to the properties of the individual (noninteracting) components. The appearance of a characteristic peak of the partial structure factor of the polymer component indicates redistribution of segment density. This result is consistent with our calculations. In Figure 21 we compare the changes predicted by theory in the behavior of the function $\hat{S}_{\mathrm{pp}}(q)$ with the corresponding experimental curve of neutron scattering intensity $I_{\mathrm{pp}}(q) \sim \rho_{\mathrm{p}} V \hat{S}_{\mathrm{pp}}(q)$. As can be seen, in both cases the adsorption effects drastically reduce compressibility and result in the appearance of the peak on the curves. This indicates formation of quasiregular structures. According to reference [69], the characteristic size of the structure varied from 5 to 15 nm depending on polymer concentration. According to our calculations, as temperature decreases the q^+ peak of the polymer component appears at $q \approx 0.75/\sigma_{\mathrm{p}}$ and shifts gradually to $q \approx 1.8/\sigma_{\mathrm{p}}$. These estimates for the period of the structure are consistent with the experimental data (if, according to Sect. 2, $\sigma_{\mathrm{p}} \approx 1$ nm). According to reference [69], with PEO concentration increasing the q^+ peak shifts to larger q. The same tendency is observed in Figure 18.

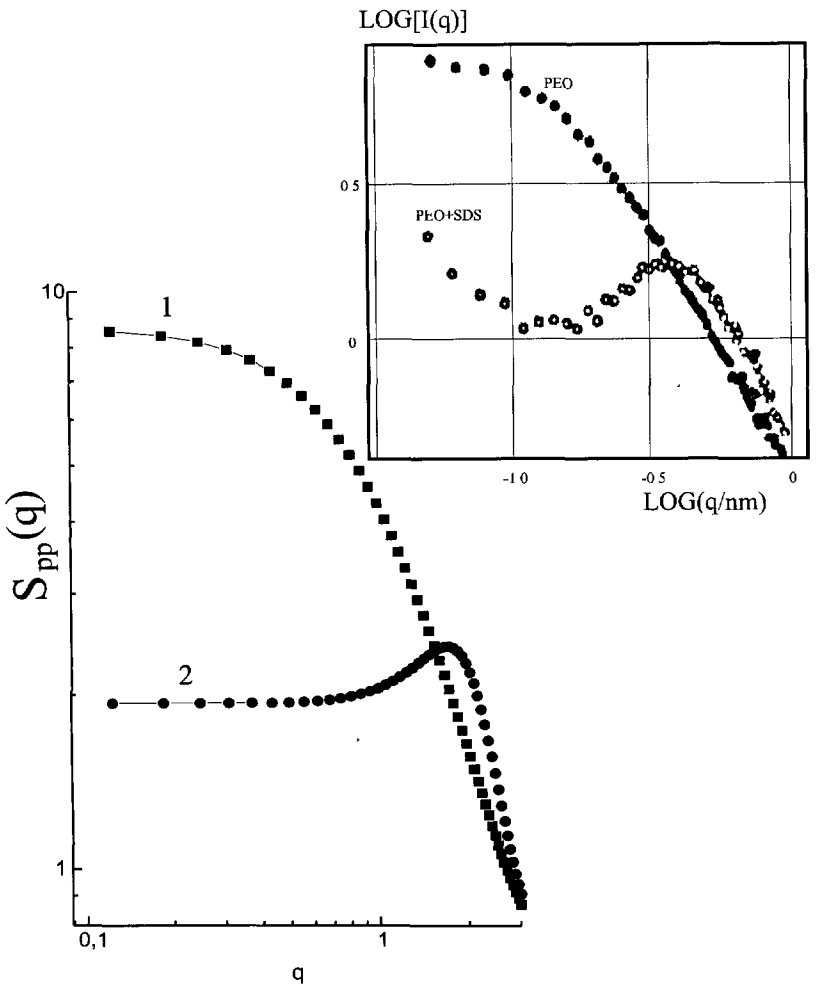

Fig. 21. — The scattering functions for the polymer chains; curve 1: without consideration of adsorption on particles; curve 2: with accounting for adsorption that results in the appearance of a quasiperiodic structure ($T = 2.5$; $\rho_d = 0.02$; $\rho_p = 0.8$). The logarithmic scale is used. The inset figure shows the corresponding experimental data [69].

4.8. The Diagram of States. — We summarize the results of calculations in Figure 22, which gives a schematic representation of the complete diagram of states of the system in the coordinates: *temperature — polymer volume fraction* (density of particles is assumed to be fixed). The dotted lines in the diagram are the curves of quasiideal behavior of the colloidal component. On these curves the reduced compressibility of particles $\chi^* \equiv \hat{S}_{dd}(0)$ is the same as of the ideal gas ($\chi^* = 1$). In the region A, which lies between the upper and lower curves of quasiideal behavior, we have $\chi^* < 1$. In two regions B that lie above the upper curve and below the lower curve we have $\chi^* > 1$. In the subregion S, which is a constituent of the region A, the conditions of the increased stability of the dispersion are realized. In the subregion S compressibility is considerably lower, as compared to the system of individual particles at the same density, *i.e.*, stable adsorption complexes are formed because of linking

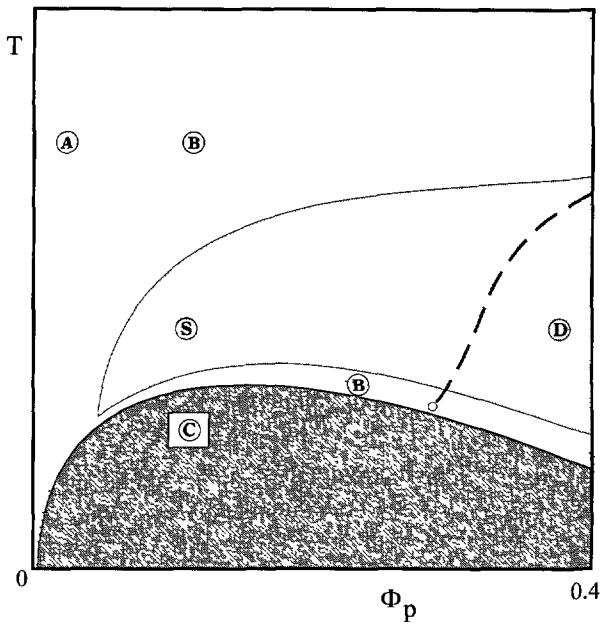

Fig. 22. — The calculated schematic state diagram of the subsystem of colloidal particles in the coordinates: *temperature — polymer volume fraction.*

together chains and particles. On the boundaries of the subregion S the polymer additives do not affect compressibility of the colloidal dispersion. In the region C intensive aggregation of particles occurs. This is due to their effective attraction mediated by strong adsorption of chains. In this case a singularity of χ^* is observed ($\chi^* \to \infty$). The dashed line that begins at the boundary of the subregion C defines the region D, where packing of stable adsorption complexes results in formation of quasiregular structures with periodic alternating of particles and polymer segments. Note that the diagram of states presented in Figure 22 corresponds to a semidilute polymer solution and does not describe the behavior of the system at higher concentrations of the polymer.

5. Conclusion

A detailed study of interaction of small spherical particles with polymer chains in the regimes of strong and weak adsorption of macromolecules on the surface of the particles is performed on the basis of the RISM integral equation theory. The temperature and concentration regions characterized by different effect of the polymer on the stability of the colloidal dispersion are determined. The conditions of formation of thermodynamically stable quasiregular structures are established. The corresponding temperature–concentration state diagrams are constructed.

Acknowledgments

Financial support of the E.I. Dupont de Nemours Company is gratefully acknowledged. This work was also supported (in part) by the Russian Foundation for Fundamental Researches (Grant # 95-03-08170a).

References

[1] Napper D.H., Polymeric Stabilization of Colloidal Dispersions (Academic Press, London, 1983).

[2] Cabane B., in Colloids at Interfaces, M. Veyssie and A. Cazabat, Eds. (Editions de Physique, France, 1984).

[3] Surface and Colloid Science, R. Matijeric, Ed. (Wiley–Interscience, New York, 1976); Goodwin J.W., in Colloid Science, D.H. Everett, Ed., Vol. 2, Chap. 7 (Chemical Society, London, 1976); Baran A.A., Polimersoderzhashchie dispersnye sistemy, "Polymer–Containing Dispersed Systems" (Naukova Dumka, Kiev, 1986).

[4] de Gennes P.–G., Scaling Concepts in Polymer Physics (Ithaca, Cornell Univ. Press, 1979).

[5] Asakura S. and Oosawa F., *J. Chem. Phys.* **22** (1954) 1255; *J. Polym. Sci.* **33** (1958) 183.

[6] Fischer E.W., *Kolloid Z.* **160** (1958) 120; Meier D.J., *J. Phys. Chem.* **71** (1967) 1861.

[7] Jäckel K., *Kolloid Z.* **197** (1964) 143.

[8] Clayfield E.J. and Lumb E.C., *J. Colloid Interface Sci.* **22** (1966) 269, 285.

[9] Lyklema J., *Adv. Colloid Int. Sci.* **2** (1968) 65.

[10] Hesselink Th.F., *J. Phys. Chem.* **75** (1971) 65.

[11] Hesselink Th.F., Vriij A. and Overbeek F.Th.G., *J. Phys. Chem.* **75** (1971) 2094.

[12] Vincent B., *Adv. Colloid Int. Sci.* **4** (1974) 193.

[13] Dolan A.K. and Edwards S.F., *Proc. Roy. Soc. London* **337** A (1974) 509.

[14] Osmond D.W.J., Vincent B. and Waite F.A., *Colloid Polymer Sci.* **253** (1975) 676.

[15] Alexander S., *J. Phys. France* **38** (1977) 977.

[16] Daoud M. and de Gennes P.–G., *J. Phys. France* **38** (1977) 85.

[17] Joanny J.F., Leibler L. and de Gennes P.–G., *J. Polym. Sci. Polym. Phys. Ed.* **17** (1979) 1073; de Gennes P.–G., *C. R. Acad. Sci. (Paris)* **289** B (1979) 103.

[18] Gerber P.R. and Moore M.A., *Macromolecules* **10** (1977) 476,

[19] Feigin R.I. and Napper D.H., *J. Colloid Int. Sci.* **75** (1980) 525.

[20] Klein J. and Pincus P., *Macromolecules* **15** (1982) 1129.

[21] Sperry P.R., *J. Colloid Int. Sci.* **87** (1982) 375.

[22] Gast A.P., Hall C.K. and Russel W.B., *J. Colloid Int. Sci.* **96** (1983) 251.

[23] Gast A.P., Hall C.K. and Russel W.B., *Faraday Discuss. Chem. Soc.* **76** (1983) 189.

[24] Khalatur P.G., *Kolloid Zh.* **45** (1983) 821, 975; *ibid.* **46** (1984) 517.

[25] Pincus P.A., Sandroff C.J. and Witten T.A., *J. Phys. France* **45** (1984) 725.

[26] Cates D.L. and Hirtzel C.S., *J. Colloid Int. Sci.* **120** (1987) 404.

[27] Halperin A., *Europhys. Lett.* **4** (1987) 439.

[28] Vincent B., *Colloids Surf.* **24** (1987) 269.

[29] Vincent B., Edwards J., Emmett S. and Croot R., *Colloids Surf.* **31** (1988) 267.

[30] Fleer G.J., Scheutjens J.M.H.M. and Cohen Stuart M.A., *Colloids Surf.* **31** (1988) 1.

[31] Marques C.M. and Joanny J.F., *J. Phys. France* **49** (1988) 1103.

[32] Attard P., *J. Chem. Phys.* **91** (1989) 3083.

[33] Canessa E., Grimson M.J. and Silbert M., *Mol. Phys.* **67** (1989) 1153.

[34] Santore M.M., Russel W.B. and Prud'homme R.K., *Macromolecules* **23** (1990) 3821.

[35] Klimov D.K. and Khokhlov A.R., *Polymer* **33** (1992) 2177.

[36] Flory P.J., Principles of Polymer Chemistry (Ithaca, N.Y., Cornell University Press, 1953).

[37] Sillberberg A., *J. Chem. Phys.* **46** (1967) 1105; *ibid.* **48** (1968) 2835.

[38] Hoeve C.A.J., *J. Polym. Sci. C* **30** (1970) 361; *ibid. C* **34** (1971) 1.

[39] Roe R.J., *J. Chem. Phys.* **60** (1974) 4192.
[40] Helfand E., *J. Chem. Phys.* **63** (1975) 2192.
[41] Helfand E., *Macromolecules* **9** (1976) 307.
[42] Levine S., Thomlinson M.M. and Robinson K., *Discuss. Faraday Soc.* **65** (1978) 202.
[43] Scheutjens J.M.H.M. and Fleer G.J., *J. Phys. Chem.* **83** (1979) 1619; *ibid.* **84** (1980) 178.
[44] Khalatur P.G. and Pavlov A.S., *Vysokomol. Soed. A* **25** (1983) 1697; *ibid. A* **25** (1983) 2599.
[45] Khalatur P.G., *Kolloid. Zh.* **46** (1984) 294.
[46] Eichinger B.E., Jackson D.M. and McKay B.D., *J. Chem. Phys.* **85** (1986) 5299; *ibid.* **88** (1988) 517.
[47] Myers K.R., Nemirovski A.M. and Freed K.F., *J. Chem. Phys.* **97** (1992) 2790.
[48] Myers K.R. and Freed K.F., *J. Chem. Phys.* **98** (1993) 2437.
[49] Allegra G. and Colombo E., *J. Chem. Phys.* **98** (1993) 7398; *ibid.* **105** (1996) 3801.
[50] Yethiraj A. and Hall C.K., *J. Chem. Phys.* **95** (1991) 3749.
[51] Yethiraj A., Hall C.K. and Dickman R., *Colloid Int. Sci.* **151** (1992) 102.
[52] Curro J.G. and Schweizer K.S., *J. Chem. Phys.* **87** (1987) 1842.
[53] Schweizer K.S. and Curro J.G., *Adv. Polymer Sci.* **116** (1994) 319.
[54] Schweizer K.S. and Curro J.G., *Adv. Chem. Phys.* (1996) in press.
[55] Henderson D., Abraham F.F. and Barker J.A., *Mol. Phys.* **31** (1975) 1291.
[56] Zhou Y. and Stell G., *Mol. Phys.* **66** (1989) 767.
[57] Walley A., Schweizer K.S., Peanasky J., Cai L. and Granick S., *J. Chem. Phys.* **100** (1994) 3361.
[58] Chandler D., McCoy J.D. and Singer S.J., *J. Chem. Phys.* **85** (1986) 5971, 5977.
[59] McMullen W.E. and Freed K.F., *J. Chem. Phys.* **92** (1990) 1413.
[60] Woodward C.E., *J. Chem. Phys.* **94** (1991) 3183; *ibid.* **97** (1992) 695; *ibid.* **97** (1992) 4525;
[61] Kierlik E. and Rosinberg M.L., *J. Chem. Phys.* **97** (1992) 9222; *ibid.* **99** (1993) 3950; *ibid.* **100** (1994) 1716.
[62] Sen S., Cohen J., McCoy J.D. and Curro J.G., *J. Chem. Phys.* **101** (1994) 9010.
[63] Sen S., McCoy J.D., Nath S.K., Donley J.P. and Curro J.G., *J. Chem. Phys.* **102** (1995) 3431.
[64] Donley J.P., Rajasekaran J.J., McCoy J.D. and Curro J.G., *J. Chem. Phys.* **103** (1995) 5061.
[65] Donley J.P., Curro J.G. and McCoy J.D., *J. Chem. Phys.* **101** (1994) 3205.
[66] Woodward C.E. and Yethiraj A., *J. Chem. Phys.* **100** (1994) 3181.
[67] Phan S., Kierlik E., Rosinberg M.L., Yethiraj A. and Dickman R., *J. Chem. Phys.* **102** (1995) 2141.
[68] Yethiraj A. and Woodward C.E., *J. Chem. Phys.* **102** (1995) 5499.
[69] Cabane B. and Duplessix R., *J. Phys. France* **48** (1987) 651.
[70] Cabane B., *J. Phys. Chem.* **81** (1977) 1639.
[71] Cabane B. and Duplessix R., *J. Phys. France* **43** (1982) 1529.
[72] Cabane B. and Duplessix R., *Colloids Surf.* **13** (1985) 19.
[73] Gruen D.W.R., *J. Colloid Int. Sci.* **84** (1981) 281; *Progr. Colloid Polym. Sci.* **70** (1985) 6.
[74] Chandler D. and Andersen H.C., *J. Chem. Phys.* **57** (1972) 1918, 1930; Chandler D., in "Studies in Statistical Mechanics VIII", E.W. Montroll and J.L. Lebowitz, Eds. (Amsterdam, North–Holland. 1982) pp. 275–340.
[75] Croxton C.A., Liquid State Physics — A Statistical Mechanical Introduction, Cambridge (Cambridge University Press, 1974).

[76] Hansen J.P. and McDonald I.R., Theory of Simple Liquids, 2nd ed. (Academic Press, London, 1986).
[77] Schweizer K.S. and Curro J.G., *Phys. Rev. Lett.* **58** (1987) 246.
[78] Genz U. and Klein R., *J. Phys. France* **50** (1989) 439.
[79] Genz U., Klein R. and Benmouna M., *J. Phys. France* **50** (1989) 449.
[80] Benmouna M. and Grimson M.J., *Macromolecules* **20** (1987) 1161.
[81] Grimson M.J., Benmouna M. and Benoit H., *J. Chem. Soc., Faraday Trans. 1* **84** (1988) 1563.
[82] Lovesey S.W., The Theory of Neutron Scattering from Condensed Matter, Vol. 1 (Claredon Press, Oxford, 1984); Pings C.J., in "Physics of Simple Liquids", H.N.V. Temperley, *et al.*, Eds., (North–Holland Publ. Co., Amsterdam, 1968).
[83] Schweizer K.S. and Curro J.G., *J. Chem. Phys.* **91** (1989) 5059.
[84] Schweizer K.S. and Curro J.G., *Macromolecules* **21** (1988) 3070.
[85] Yamakawa H., Modern Theory of Polymer Solutions (Harper and Row, New York, 1971).
[86] Chandler D. and Pratt L.R., *J. Chem. Phys.* **65** (1976) 2925.
[87] Pratt L.R. and Chandler D., *J. Chem. Phys.* **65** (1976) 147.
[88] Chandler D., Singh Y. and Richardson D.M., *J. Chem. Phys.* **81** (1984) 1975.
[89] Nichols A.L., Chandler D., Singh Y. and Richardson D.M., *J. Chem. Phys.* **81** (1984) 5109.
[90] Schweizer K.S., Honnell K.G. and Curro J.G., *J. Chem. Phys.* **96** (1992) 3211.
[91] Malenkewitz J., Schweizer K.S. and Curro J.G., *Macromolecules* **26** (1993) 6190.
[92] Grayce C.J. and Schweizer K.S., *J. Chem. Phys.* **100** (1994) 6846.
[93] Grayce C.J., Yethiraj A. and Schweizer K.S., *J. Chym. Phys.* **100** (1994) 6857.
[94] Talitskich S.K. and Khalatur P.G., *Russ. J. Phys. Chem. 67* (1993) 412.
[95] Khalatur P.G., *Russ. Phys. Bull.* **59** (1995) 178.
[96] Khalatur P.G. and Khokhlov A.R., in preparation.
[97] Yethiraj A. and Schweizer K.S., *J. Chem. Phys.* **97** (1992) 1455.
[98] Schweizer K.S. and Yethiraj A., *J. Chem. Phys.* **98** (1993) 9053.
[99] Yethiraj A. and Schweizer K.S., *J. Chem. Phys.* **98** (1993) 9080.
[100] Lowden L.J. and Chandler D., *J. Chem. Phys.* **59** (1973) 6587; *ibid.* **61** (1974) 5228.
[101] Chandler D., *J. Chem. Phys.* **59** (1973) 2742.
[102] Ohba M. and Arakawa K., *J. Phys. Soc. Jpn* **55** (1986) 2955.
[103] Gromov D.G. and de Pablo J.J., *J. Chem. Phys.* **103** (1995) 8247.
[104] Talitskikh S.K. and Khalatur P.G., *Russ. J. Phys. Chem.* **69** (1995) 5.
[105] Makeeva I.V., Kokacheva V.G., Talitskikh S.K. and Khalatur P.G., *Russ. J. Struct. Chem.* **36** (1995) 799.
[106] Rushbrooke G.S., in "Physics of Simple Liquids", H.N.V. Temperley, *et al.*, Eds. (North–Holland Publ. Co., Amsterdam, 1968) chapter 2.
[107] Scheutjens J.M.H.M. and Fleer G.J., *Adv. Colloid Int. Sci.* **16** (1982) 361.
[108] Wigner E., *Phys. Rev.* **46** (1934) 1002.
[109] Foldi L., *Phys. Rev. B* **3** (1971) 3472.
[110] Schwarz H.A., Gesammelte Mathematische Abhandlung (Springer, Berlin, 1890) Band 1, pp. 6–125.
[111] Scriven L.E., *Nature* **263** (1976) 123.